386 c

POWER SPECTRAL ANALYSIS OF A FORCEMAIN FAILURE CAUSED BY WATERHAMMER

POWER SPECTRAL ANALYSIS OF A FORCEMAIN FAILURE CAUSED BY WATERHAMMER

June, 1977

by

Robert R. Hennessy, B.A.Sc, P.Eng.

A PROJECT

Submitted to the School of Graduate Studies of
McMaster University

in partial fulfilment of the requirements

for the Degree of Master of Engineering

Master of Engineering (1977) McMaster University

(Civil Engineering) Hamilton, Ontario.

Title: Power Spectral Analysis of a Forcemain Failure Caused by Waterhammer

Author: Robert R. Hennessy, B.A.Sc., University of Waterloo

Supervisor: Dr. William James

Number of Pages: VI, 67

INDEX

LIST OF FIGURES

ABSTRACT

The failure of the Ancaster forcemain was thought to be related to waterhammer effects. The sequence of breakages of the main are reviewed. A series of pressure recordings were made on the forcemain, leading up to and including collapse. The recordings comprise a unique data set.

These pressure recordings were digitized and subjected to power spectral analysis. The power spectra pointed out several significant events that were not evident from the pressure record alone.

These included the fact that the original break occurred in the forcemain several days prior to its ultimate collapse and discovery on the surface. It was also determined that the break in the pipe was due to the apparent merging of the primary waterhammer wave with an existing but gradually changing lower frequency wave. This second wave was associated with rigid column motion and gradually increased its frequency. The resultant wave carried sufficient energy to cause the ultimate failure of the evidently already damaged forcemain.

Power spectral analysis proved useful as a method for analysing waterhammer effects in a forcemain complicated by column separation, leakage and vapour pocket collapse, and may be a useful way of monitoring the performance of longer pipelines.

ACKNOWLEDGEMENTS

The author would like to acknowledge and thank the following people for their invaluable assistance in preparing this report.

Dr. William James, P.Eng.
Professor of Civil Engineering
McMaster University
Hamilton, Ontario
- For suggesting the problem, providing the data, supervision and technical guidance.

Mr. Jerry Discher, P.Eng.
Manager of Municipal & Highway Department
C. C. Parker and Associates
Consulting Engineers
Hamilton, Ontario
- For information on the history and physical aspects of the forcemain.

Mrs. Irene Watson
Secretary
The Hamilton Harbour Commissioners
Hamilton, Ontario
- For typing this report.

1. INTRODUCTION

1.1 PURPOSE

In this study, power spectral analysis is applied to a series of pressure recordings in a forcemain to interpret the failure of the pipeline.

The pressure surges or waves in the forcemain were caused by the stoppage of a pump.

The pressure recordings were taken over a period of 14 days and include collapse of the pipe; they provide a unique data set for study of the waterhammer problem. This is probably also the first study to apply power spectral analysis to interpret waterhammer failure in a forcemain.

1.2 REVIEW OF WATERHAMMER

Waterhammer is the name given to the phenomenon of pressure waves travelling back and forth in a pipe flowing full. These pressure waves are caused by a change of velocity in the pipe. A change in velocity at a point in a fluid always results in a pressure change. Waterhammer is a result of this pressure change and is due to inertial and elastic effects. Thus the pressure surges are greater in large diameter and long pipes, especially if carrying a high discharge; and in inelastic pipes.

Rapid velocity changes in a pipe are usually the result of closing or opening a valve, or of stopping or starting a pump. The resulting pressure waves travel up and down the pipe at the speed of sound in the elastic fluid and pipe. In metal pipes this process may produce a noise -- hence the term "waterhammer".

In waterhammer the elasticity of both the pipe and the fluid are important. Because of this elasticity the pressure change does not occur instantaneously everywhere in the pipe, but instead is propagated as a wavefront.

The process is illustrated as follows:

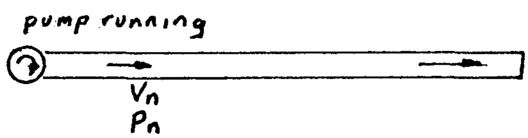

- pump running normally
- pipe flowing full at velocity V_n

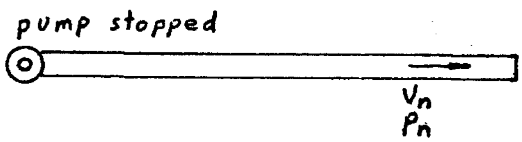

- pump stopped suddenly (assumed instantaneous stoppage for this illustration)
- pipe continues to flow full at velocity V_n
- not enough fluid at pump available to maintain flow

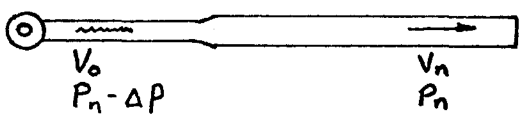

- low pressure develops and will bring fluid to rest
- pipe wall contracts
- fluid expands

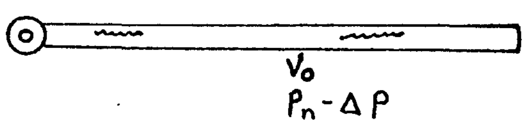

- process travels downstream, bringing all fluid to rest
- if pressure is reduced below vapour pressure at a point in line, fluid vapourizes and downstream column continues to move but at a slower rate
- process of each successive portion of fluid coming to rest appears as a negative pressure wave moving downstream.
- at this instant momentum is zero and all kinetic energy has been converted to elastic energy

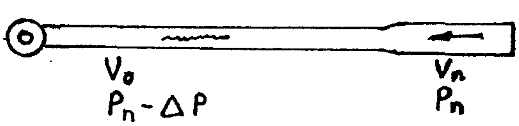

- system is unbalanced at end of pipe
- fluid flows back in low pressure zone in pipe
- pressure returns to normal

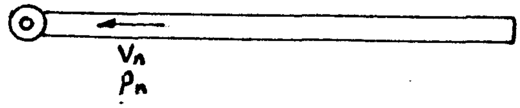

- process reaches pump
- pressure is normal
- velocity now V_n in reverse direction

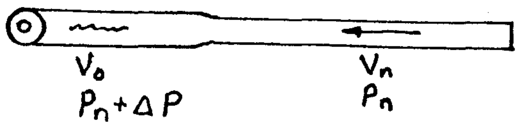

- fluid cannot get through pump (usually check valve in front of pump)
- fluid at pump comes to rest
- pressure increases
- pipe wall expands
- fluid compresses

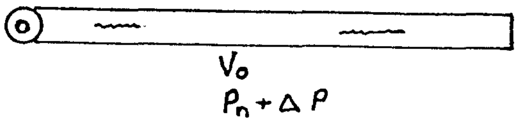

- process continued in reverse direction
- fluid comes to rest and pressure increases

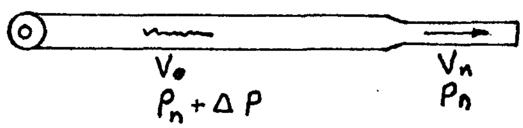

- at open end fluid is under pressure and starts to flow from pipe at V_n
- pipe wall contracts
- pressure is normal

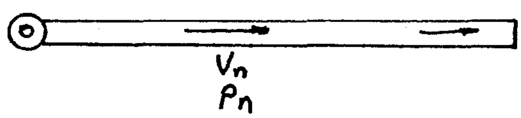

- process proceeds towards pump
- flow is V_n out of pipe
- pressure is normal
- at pump there is no fluid to maintain flow and entire cycle begins again.

FIG. I

Note that the process repeats after travelling up and down the pipe twice, a distance of four (4) times the pipe length.

Now, consider the pressure at a point in the pipe near the pump, as the pressure wave moves up and down the pipe. The local cycle of pressure change appears as a square pressure wave, if we neglect the effect of the inertia of the rotating mass and also the finite closure time of the check valve.

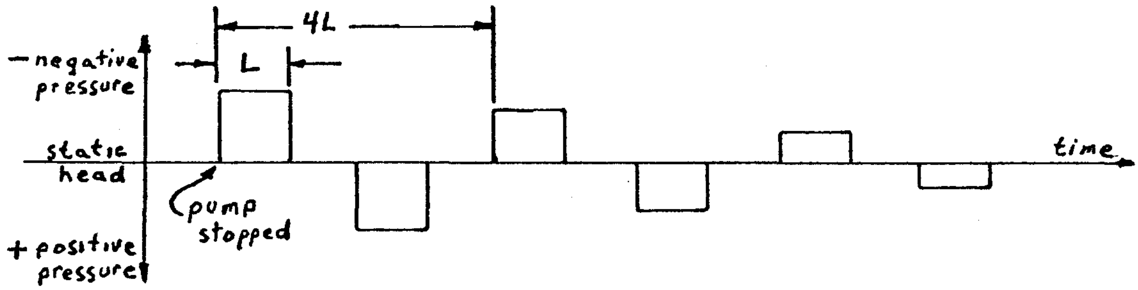

THEORETICAL WATERHAMMER WAVE

FIG. II

In practice, the amplitude of the wave is damped out because of fluid friction and imperfect elasticity in the fluid and pipe wall. Also, because of pump inertia, the actual curve appears to be sinusoidal. After a few cycles the fluid comes to rest under the static head or the normal operating head, as the case may be. The period of the wave is a function of the pipe length since the recurrence of the wave is dependent upon its reflection at the end of the pipe. If the celerity of the pressure wave is "a" and the length of the pipe is "L" then the period of the pressure wave is $\frac{4L}{a}$.

The process can be expressed mathematically by analysing a control volume of fluid in a pipe in terms of continuity of flow.

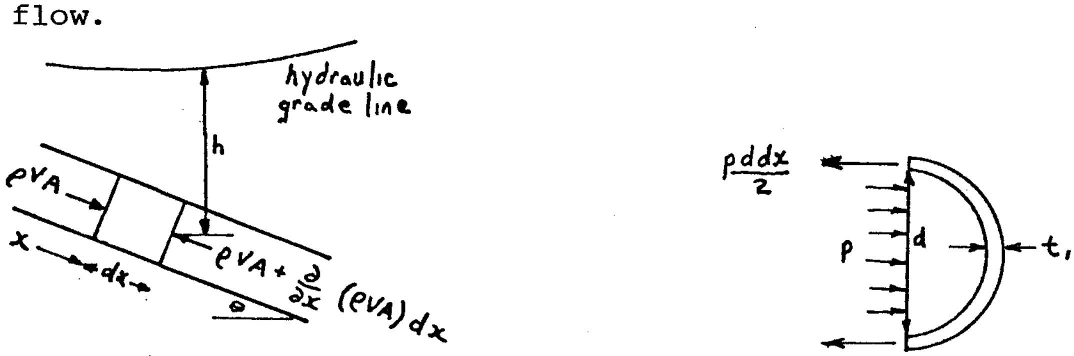

PIPE LENGTH PIPE CROSS SECTION

FIG.III

For continuity we know that Inflow- Outflow= Rate of change of volume (storage).

Now Inflow = ρVA

Outflow = $\rho VA + \frac{\partial}{\partial x}(\rho VA)\,dx$

Volume change due to pipe elasticity

Rate of Stress Change = $\frac{d}{2t_1}\frac{\partial p}{\partial t}$

Strain Rate = $\frac{d}{2t_1E}\frac{\partial p}{\partial t}$

Rate of Volume Increase = $\frac{\pi d^3}{4t_1E}\,dx\,\frac{\partial p}{\partial t}$

Volume change due to fluid compressibility

Rate of Volume Increase = $\frac{\pi d^3}{4K}\,dx\,\frac{\partial p}{\partial t}$

where K is fluid bulk modulus

$$K = -\frac{\partial p}{\partial V/V}$$

Therefore, for continuity

$$\rho VA - \left(\rho VA + \frac{\partial}{\partial x}(\rho VA)\,dx\right) = \left(\frac{\pi d^3 dx}{4t_1E} + \frac{\pi d^2 dx}{4K}\right)\frac{\partial p}{\partial t}$$

This can be simplified to

$$\frac{\partial h}{\partial t} + \frac{a^2}{g}\frac{\partial V}{\partial x} = 0$$

where a = celerity of the pressure wave

$$a = \frac{1}{\sqrt{w/g\,(1/K + d/t_1E)}}$$

By normalizing, setting up a time space grid and solving along the characteristics $\frac{d X_0}{d T_0} = \pm 1$ this equation can be solved with no numerical instability. Several computer programs are available for this purpose.[1,2]

Thus the wave period is related directly to pipe length, wall thickness, pipe elasticity and the density and elasticity of the fluid:

$$\text{Period} = \frac{4L}{a}$$

$$= \frac{4L}{\dfrac{1}{\sqrt{w/g\,(1/K + d/t_{,E})}}}$$

$$= 4L\left(\sqrt{w/g\,(1/K + d/t_{,E})}\right)$$

Note also that the wave frequency is the reciprocal of the period:

$$\text{frequency (hertz)} = \frac{1}{\text{period (seconds)}}$$

On the other hand the amplitude of a wave is generally directly related to the momentum quantities: rate of stoppage, velocity, diameter, length, reflectivity, transmissivity etc.

1.3 REVIEW OF POWER SPECTRAL ANALYSIS

The power spectral density function is usually plotted as the variance of a process in terms of frequency. It can be compared to the auto-correlation function which is the variance of a process with respect to time.

The power spectral density function is defined as the average power of a process expressed as a function of frequency. In wave mechanics the spectrum is plotted such that the average power of the wave process is the area under the single sided power density spectrum between two specified frequencies.

There are several methods for calculating power spectra, but the currently popular method uses the fast fourier transform.

Given a function of time, its fourier transform is a function of frequency. This method is very suitable for calculating power spectra.

The total average power of some time series $y(t)$ is

$$\bar{P}_y = \lim_{T\to\infty} \frac{1}{T} \int_{t=0}^{T} y^2(t)\,dt$$

and the power between frequency ω_0 and $\Delta\omega$ is

$$\bar{P}_y(\omega_0,\Delta\omega) = \lim_{T\to\infty} \frac{1}{T} \int_{t=0}^{T} y^2(t,\omega_0,\Delta\omega)\,dt$$

Then the power spectral density is

$$F_y(\omega_0) = \lim_{\Delta\omega\to 0} \frac{\bar{P}(\omega_0,\Delta\omega)}{\Delta\omega}$$

By expanding $F_y(\omega_0) = \lim_{\Delta\omega\to 0} \lim_{T\to\infty} \frac{1}{\Delta\omega} \frac{1}{T} \int_{t=0}^{T} y^2(t,\omega_0,\Delta\omega)\,dt$

as $T\to\infty$, $\Delta\omega = 2\pi/T \to 0$

and $F_y(\omega_0) = \lim_{T\to\infty} \frac{1}{2\pi} \int_{t=0}^{T} y^2(t,\omega_0,\Delta\omega)\,dt$

Then using fourier transform we know that

$$y(t,\omega_0,\Delta\omega) = C(\omega_0)\,e^{i\omega_0 t}\,\Delta\omega$$

and $$C(\omega_0) = \int_{t=-\infty}^{\infty} y(t)\,e^{-i\omega_0 t}\,dt$$

Thus we can calculate $F_y(\omega_0)$ for all values of ω by using a number of fourier transform pairs.

These pairs are:

1) Autocovariance function

$$C(\tau) = \frac{1}{2\pi} \int_{\omega=-\infty}^{\infty} F(\omega)\,e^{i\omega\tau}\,d\omega$$

2) Power spectral density funtion

$$F(\omega) = \int_{\tau=-\infty}^{\infty} C(\tau)\,e^{-i\omega\tau}\,d\tau$$

For engineering purposes we eliminate the negative frequencies and get the single sided power spectral density function

$$S(\omega) = 2 \int_{\tau=-\infty}^{\infty} C(\tau)\, e^{-i\omega\tau}\, d\tau$$

Since $C(\tau) = C(-\tau)$ and $S(\omega)$ must be real,

we have

$$S(\omega) = 4 \int_{\tau=0}^{\infty} C(\tau) \cos \omega\tau \, d\tau$$

This is the equation solved by the program in order to obtain the power spectrum.

Note that $S(\omega)$ as obtained by the above process is only an estimated value. The real value of $S(\omega)$ would require an infinitely long data set.

2. THE ANCASTER FORCEMAIN

2.1 BRIEF HISTORY

The forcemain was constructed about two years ago to pump raw sewage from a wet well near the old Ancaster Road to the main gravity sewer, on Lowden Avenue. The line was originally constructed of 14 inch diameter class 100 asbestos cement pipe. It is 3,963 feet long and rises a total of 133 feet. A profile of the line is shown in Fig. IV.

There was some question at the time of construction as to whether proper pressure testing was carried out. The pump was first started in the fall of 1975. Shortly thereafter a leak occurred about 150 feet downstream from the pump. The pipe was excavated, and the leak found to be the result of a broken coupling. The pipe was repaired, the trench refilled, and the pump restarted.

In a short time another leak was detected. It was found that the coupling downstream from the first break had also broken. It was subsequently repaired and the pump restarted.

The line broke again at the next coupling down the line. These three couplings were located adjacent to a stream. It was believed that the breaks were the result of settlement of the pipeline resulting from the poor soil condition in this area.

After the third break about 150 lineal feet of line in the area of the breaks was replaced with ductile iron pipe.

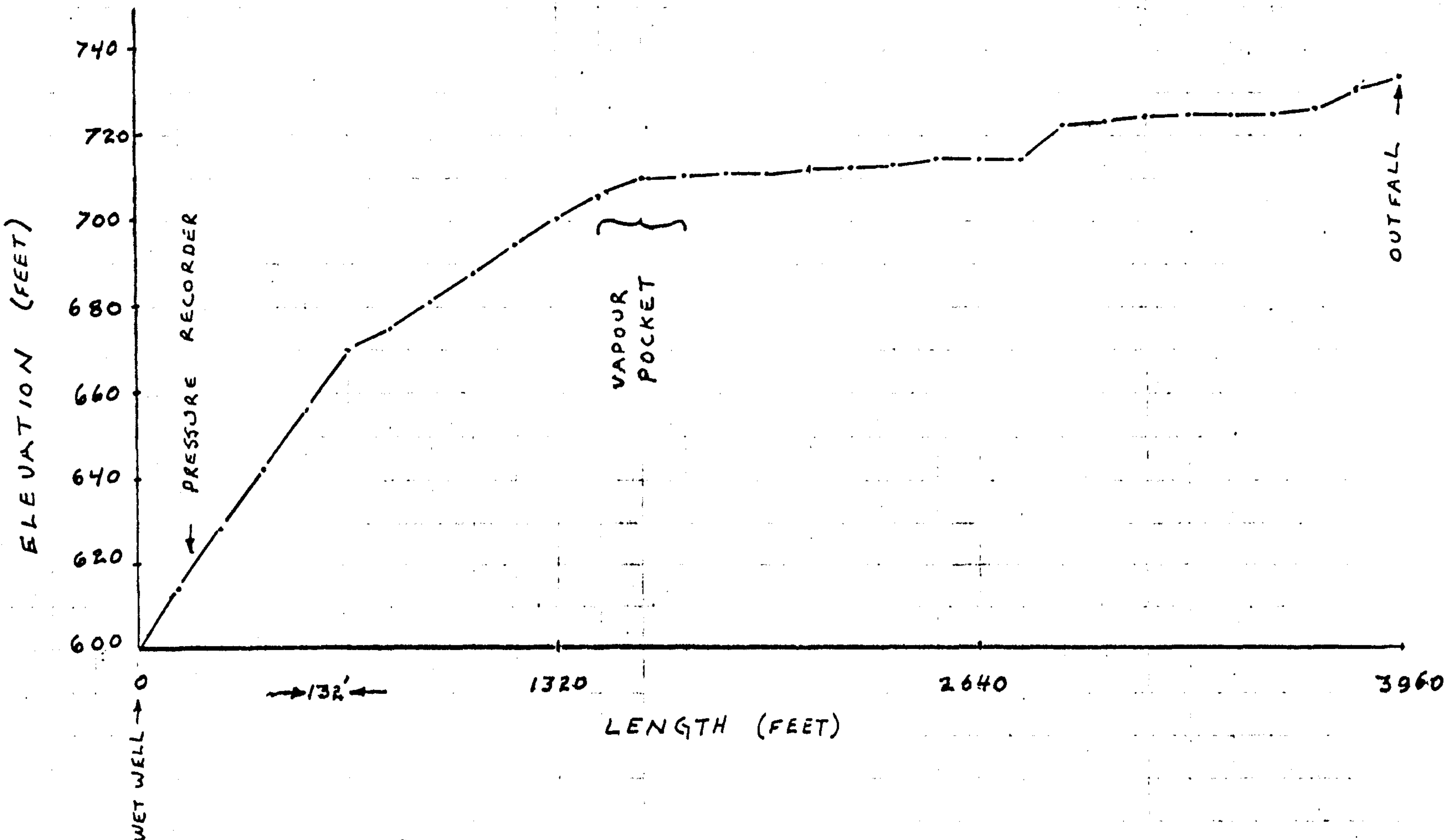

PROFILE OF ANCASTER FORCEMAIN

FIG. IV

The entire line was then pressure tested and found to meet required standards. The system was started again in August, 1976. The pipeline broke again on September 14th, 1976. At this time it was thought that the breakage problem was caused by waterhammer effects coupled with pipe settlement. It was known that vapour pockets were forming in the line. Therefore, protective pressure vessels were designed by Dr. W. James and installed in the forcemain system.

2.2 TEST PROCEDURE

It was determined that the forcemain required further study because of the suspected waterhammer problems, and evident poor condition of the couplings. In early September electronic pressure sensing devices were installed by Dr. James.

One device was placed in the line at the location of the three breaks. The device recorded the pressure waves that occurred on pump shut-down. In the period from September 9 to September 14, 1976 a total of 18 pressure wave recordings were made at this location. (Sample recordings are shown in Appendix 1). On September 14 the pipeline again collapsed, while the pressure recording device was operating. This provided a complete record of waterhammer pressure waves, during the deterioration of the pipe up to and including failure; a unique data set for study of waterhammer related collapse.

The latest break proved difficult to locate. It was eventually found 450 feet from the pump and again proved to be a broken coupling. The entire pipe length between the 150 and 450 foot marks was then replaced with ductile iron pipe.

A camera was used to assist in locating the break. The camera showed deposits of gravel and dirt in the pipe to a depth of approximately 4 inches immediately downstream of the break.

There were later alterations made to the forcemain that are not relevant to this study.

3. DATA PROCESSING

The data set consists of graphical records of surge waves generated by 18 separate pump stoppages. It covers the period from September 9 to September 14, 1976. The recordings are in the form of 18 separate 14" x 8½" sheets. The available sheets were copied from the output of an XY plotter that was attached to the pressure transducer. The transducer was located in the pipe approximately 150 feet downstream from the pump. The location of the transducer at a distance from the pump will produce a waterhammer pressure plot with narrower peaks than if the transducer were next to the pump[3]. However, in this case the spacing of 150 feet in relation to the total length of the pipeline is small enough that this effect can be neglected. A sample plot is shown in Fig. V.

The plotting paper travelled at a speed of 5 mm/sec while recording the pressure waves. It was only activated upon pump stoppage and continued until the waves were completely damped. The vertical scale on the plotter was set such that 1 mm represented 4.9 psi of pressure within the pipe. The reading was calibrated against static head.

The continuous plots were discretized by reading the pressure every 0.20 sec. (1 mm horizontal scale). This was accomplished by placing the plots on an electronic digitizer and automatically punching both the abcissa and ordinate of the plots onto paper tape.

The tape was then processed through a tape reader and

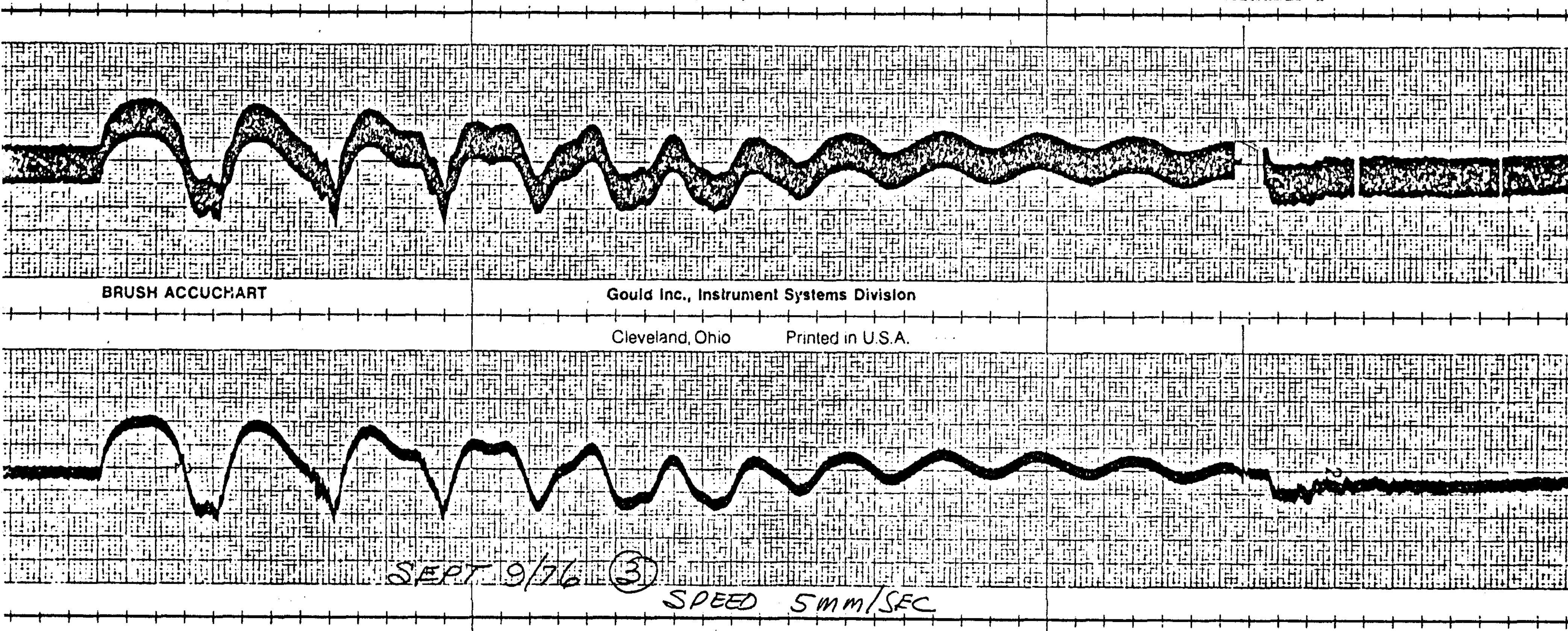

TYPICAL PRESSURE RECORD

FIG. V

stored on a permanent disk file in the CDC 6400 computer at McMaster University. Once on permanent file, the entire record, or any part thereof, could be accessed for analysis. The total record consisted of approximately 5000 data points.

The purpose of this effort was to perform a power spectral analysis on the data to determine significant frequencies in the pressure wave records.

There are several library programs available to perform spectral analysis. Two were initially investigated. These were International Mathematical and Statistical Library FTFFT1 and International Mathematical and Statistical Library FTFREQ.

The subprogram FTFFT1 was tested but the spectrum produced was not well defined. In this study the wave record caused by one pump stoppage involved approximately 200 data points. Program FTFFT1 is not suited for such short data sets.

On the other hand, the subprogram FTFREQ produces a reasonably well-defined spectrum for the short records available and was subsequently used for the analysis of the total record.

The input required for the program consists of the discretized wave data set, the time interval between readings (.20 sec) and the number of desired lags. Also available are pre-whitening and detrending routines that can be accessed with suitable input. These options were not used in this analysis.

The output from the subprogram consists of the frequencies and associated power spectra for the input data set. The number of points computed in the power spectrum corresponds to the number of lags specified in the input. In this case 90 lags were specified, with approximately the first 30 being non-zero. A sample output is shown in Fig. VI.

```
TOTAL DATA PTS,START READ,END READ
     3658       3498       3658

MEAN  AND  VARIENCE
       -3.20
     550.18
         -I
         -I
         -I
         -I
```

FREQUENCY	POWER SPECTRA
0.00	175.49
.08	319.10
.17	317.85
.25	169.13
.33	69.52
.42	27.41
.50	22.32
.58	17.38
.67	8.82
.75	3.71
.83	1.18
.92	0.00
1.00	.10
1.08	.34
1.17	.45
1.25	.59
1.33	.76
1.42	1.19
1.50	.87
1.58	.58
1.67	.38
1.75	.16
1.83	.15
1.92	.24
2.00	.20
2.08	.12
2.17	.14
2.25	.19
2.33	.16
2.42	.07
2.50	.03

TYPICAL COMPUTER OUTPUT

FIG. VI

4. RESULTS

The power spectrum produced from a waterhammer wave is affected by the shape of the waveform. The pressure record for an idealized fluid in a pipe and for instantaneous stoppage is rectangular in shape.

eg.

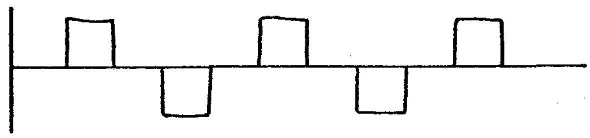

Where stoppage is affected by finite rotational momentum and valve closure times the shape tends to be saw toothed as follows:

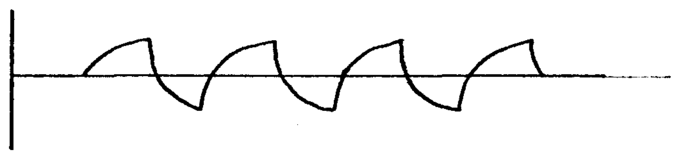

Of course, viscous effects and other frictional losses cause the waves to damp out rapidly and to assume a sinuoidal shape.

eg.

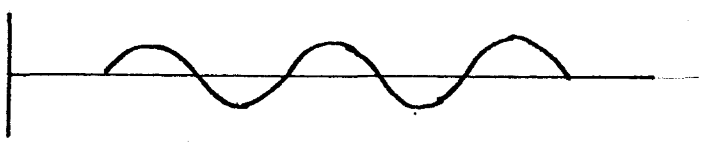

Spectral analysis of the dampened sinuoidal wave may thus produce a line spectrum

eg.

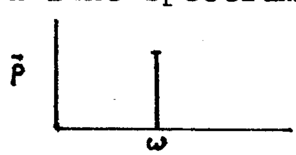

While the rectangular or saw toothed patterns will produce harmonics and other peaks in the spectra.

In this study the rotational momentum effects and valve closure times are in the order of 50% of the primary wave period. Inspection of the pressure records also indicates an absence of the rectangular and saw toothed profiles. For these reasons, the deviation of the fundamental pressure record from a sinusoidal shape has been overlooked. This aspect could be subjected to further study.

It has been found by Kassem [1] that the profile of the forcemain is such that vapour pockets will occur in the line on pump stoppage. The formation of a vapour pocket in the line will cause the pressure wave to deviate from our original illustration[2,3].

When a waterhammer pressure wave meets a vapour pocket in a line it reflects back upstream as off an open end. The downstream column decelerates and returns as a rigid column as in the case of surge tanks and other devices.

In the case of the Ancaster forcemain, the downstream end of the pipe is open. Thus a volume of water equal to the volume of the vapour pocket is lost during the first waterhammer cycle.

The expected frequencies of the waterhammer waves can thus be described as follows:

Firstly, a primary frequency can be expected to correspond with the theoretical waterhammer frequency. The observed frequency may be somewhat lower than the theoretical since the speed of the pressure wave is decreased in a partially formed vapour pocket. On the other hand it may be higher because the effective length of a partly empty and nearly horizontal pipe is reduced.

Secondly, a high frequency wave can be expected since a portion of the waterhammer pressure wave will reflect from the vapour pocket instead of travelling the entire pipe length.

Thirdly, a low frequency wave should be present to account for the rigid column motion beyond the vapour pocket.

Initially, power spectra were produced for several pressure recordings to detect how frequencies generated by a particular pump stoppage changed during the recordings. The pressure records are analysed in three portions: the first half, middle half and last half. These records are shown in Appendix IV. It was found that although the significant frequencies did not shift to any extent within specific records, the peaks on the spectral graphs diminished from the start of the record to the end. That is the first half of a record showed much higher power peaks than the last half.

This is to be expected since the power of the wave decreases during the life of the pressure waves because of imperfect elasticity and fluid friction.

Also the rate of attenuation is higher for higher frequencies than for the lower frequencies, which is also to be expected.

Of greater interest is the study of how the spectral estimates change from one pump stoppage to another. The power spectra covering the entire pressure wave caused by each pump stoppage are shown in Appendix II, Records 1 to 18.

These spectra show that the significant frequencies at the start of the record are 0.25 hertz and 0.03 hertz. These correspond to wave periods of 4 secs. and 33 secs. respectively. The 4 sec. wave is readily visible on the plots made during the test procedure.

We know that primary waterhammer wave period is calculated by: $T = \frac{4L}{a}$

$$= \frac{4\,(3963)}{\sqrt{1.94\left(\frac{1}{43.2 \times 10^6} + \frac{13.38}{0.94\,(0.49 \times 10^6)}\right)}} \text{ sec.}$$

$$= 5 \text{ sec.}$$

The observed period would be smaller because:

(1) the spectral estimate may not be "sharp" enough (i.e. the peak may actually correspond to a period in excess of 4 seconds.)

(2) the fluid properties were assumed to be those of water whereas the actual fluid contained a large amount of impurities.

(3) the pipe characteristics may vary from those used in the calculations.

(4) (2) and (3) could increase the celerity of the wave. Others [1] have calculated that the celerity is between 3400 and 3500 ft/sec. A faster celerity would give a shorter theoretical wave period (say 4.4 sec.) and hence better agreement with the power spectral estimates.

A waterhammer wave period of 4.5 secs. and phase lag of 1 sec. is plotted in Fig. VII. The actual pressure wave gives a fairly close approximation of the theoretical wave. Of course, the actual wave is not subject to the instantaneous changes characterized by the rectangular waveform dictated by instantaneous stoppage.

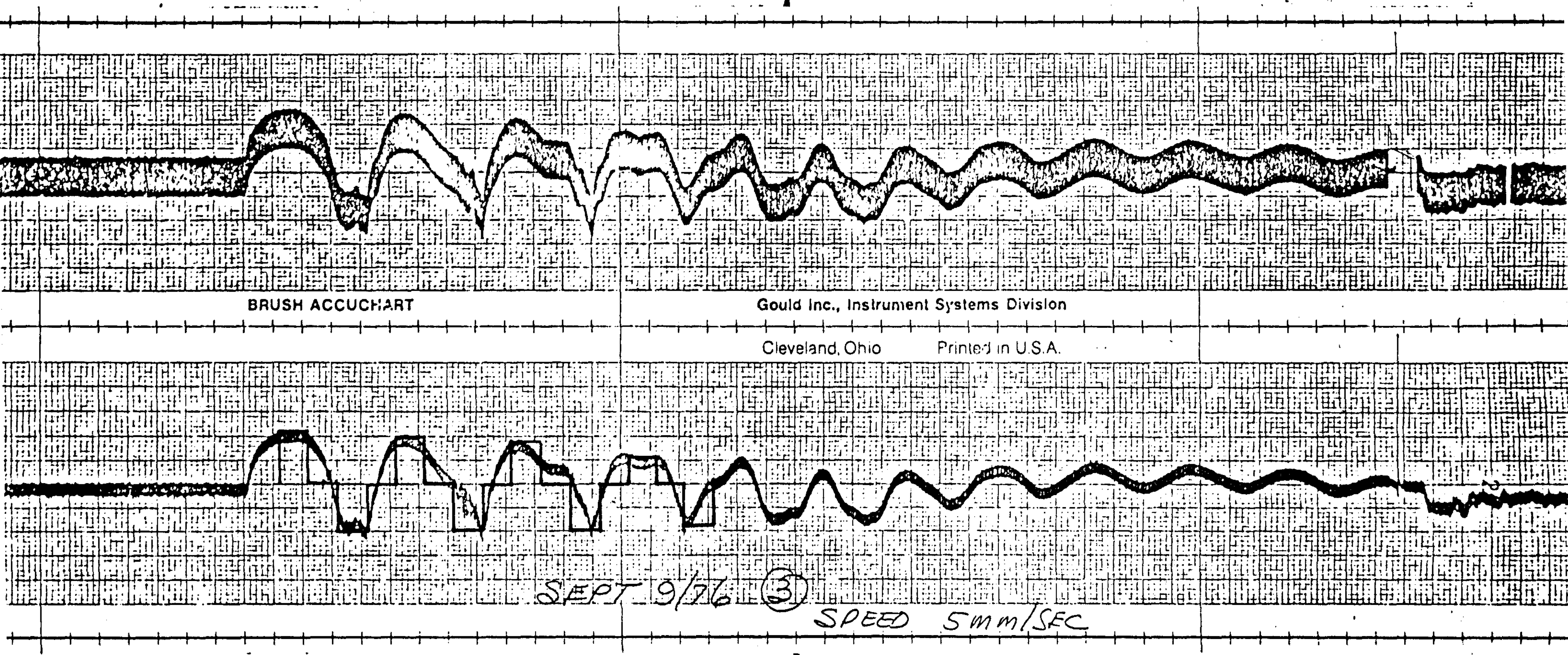

THEORETICAL WATERHAMMER WAVE
SUPERIMPOSED ON PRESSURE RECORD

FIG. VII

It is thus concluded that the peak in the spectral analysis occurring at approximately 0.25 hertz respresents the primary waterhammer wave generated by pump stoppage.

The expected high frequency peaks caused by the partial reflection of the waterhammer wave from the vapour pocket are not apparent in the power spectra. However, there are several peaks in the frequency band 0.5 to 0.8 hertz. These peaks are relatively insignificant when compared to the lower frequency peaks, but tend to confirm that part of the waterhammer wave is reflected from the vapour pocket in the pipe.

There is also a significant peak at 0.03 hertz in the power spectral estimates. This frequency corresponds to a wave period of approximately 33 secs. This wave is not easily detected in the pressure recordings. The wave period could be considerably in error since the spectral estimates are not very accurate at frequencies close to zero.

This wave is related to the expected low frequency wave formed on the downstream side of the vapour pocket. It corresponds to the back and forth motion observed at the outfall long after the pump stoppage.

Upon study of the entire record of the waterhammer plots, it is evident that commencing at plot 6 and progressing until the end of the record there is a systematic growth of one distinbct wave peak and an increasing pattern of longer period waves developing at the end of each record.

However, it is not until the 16th, 17th and 18th plots that it becomes evident that the original wave pattern has changed into a much longer period wave.

Using the spectra in Appendix II, the first spectrum clearly indicates the primary waterhammer wave at 0.25 hertz and the low frequency peak at .03 hertz representing rigid column motion.

The spectra remain relatively unchanged until spectrum No.5 where the rigid column peak becomes higher than the primary waterhammer peak. There is a considerable reduction in the magnitude of the primary waterhammer peak and a slight spreading of this peak into a higher frequency.

In spectrum 6 the 0.25 hertz wave has completely degenerated and is spread over the frequency band 0.2 to 0.4 hertz. It seems clear that a significant change in the pipeline occurred at this time. This spread of the spectrum into higher frequencies indicates that part of the wave is being reflected from a disturbance in the pipe.

The rigid column wave becomes the dominant feature in the power spectrum. The frequency of this wave increases from .03 to .06 hertz. It seems clear that the disturbance in the pipe is also affecting this wave.

The power spectra 7 through 13 remain similar to spectrum 6.

In spectrum 14 there is a significant increase in the peak of the rigid column wave. This peak has also shifted from .06 to .09 hertz. Thus the period of the wave decreases. There is also a renewed growth of the peak of the .25 hertz primary wave.

In spectra 15, 16, 17 and 18 the trend continues at an extremely fast rate. The peak of the rigid column wave on spectrum 18 has shifted to 0.11 hertz (9 sec. period) and its magnitude is 2.5 times greater than that of spectrum 14.

On the next cycle, No.19, there was a noticeable break in the pipeline and the system collapsed.

In summary, the spectral analysis shows that during the total period of the pressure records the following significant events occurred:

(1) the peak of the 0.25 hertz primary wave degenerated early in the record and was distributed into a higher frequency band.

(2) the .03 hertz (33 sec. period) rigid column wave became the dominant wave in the power spectrum.

(3) the 0.25 hertz primary wave peak reformed and grew in magnitude during the latter part of the record.

(4) the peak of the rigid column wave shifted from .03 hertz to .11 hertz during the record.

(5) the peaks of the .03 hertz rigid column wave and the .25 hertz primary wave superimposed and grew in magnitude at an extremely fast rate during the latter part of the record.

An attempt will now be made to explain these observations in terms of probable physical events in the forcemain. The collapse of the .25 hertz peak and its spread into the higher frequencies indicate that there has been a significant disturbance occurring in the pipe. The waterhammer wave is no longer travelling the entire pipe length but is being interrupted at an intermediate point. The waves are being partially reflected at this discontinuity and hence the shift in the spectrum to higher frequencies.

The phenomenon was detected using spectral analysis at the 6th record while the pipe did not actually break until the 19th record. These observations are both consistent with the effects of a broken coupling (the pipeline has a history of coupling fractures; furthermore, when the breakage was eventually repaired evidence pointed to a broken coupling as the source of the problem).

The growth and frequency shift of the low frequency wave is also consistent with the gradual increase in the magnitude of the leak or breakage at the coupling.

Any break in the forcemain would let in a volume of air during the negative surges. This air would act in the same way as a vapour pocket. With each pump stoppage the magnitude of the break would likely increase and the air volume injected would increase. Thus increased amounts of water would be ejected from the end of the pipe. This has the effect of shortening the effective length of the forcemain. A decrease in effective length of the rigid column component will decrease the period of the surge. This is also consistent with the power spectra as the low frequency wave period decreases from 33 secs. to 9 secs.

This explanation is further reinforced by the fact that while the frequency of the reflected primary pressure wave (high frequency wave) depends only on the location of the break; the frequency of the low frequency wave depends on both the location and the air volume injected at the break. A larger break will cause more water to spill from the end of the pipe, thus decreasing the effective length of the pipe and the period of the wave.

The wave transmission is further complicated by the presence of solid matter in the pipe since the pumping velocity of the forcemain is not sufficient to scour this material from the pipeline. The surges will be partially transmitted and reflected at these obstacles thereby introducing more high frequency waves.

The power spectrum indicates that the peaks of the original .03 hertz rigid column wave and the .25 hertz primary wave have merged into one .11 hertz wave at the time of breakage. This superimposition of peaks provided the energy peak required to finally fracture the coupling.

5. CONCLUSIONS

The power spectral analysis of the recorded waterhammer waves can be used to formulate a number of conclusions. Most of these conclusions could not be independently formed from a study of the pressure records alone. The conclusions, therefore, illustrate the usefulness of the technique in analysing the waterhammer records.

(1) At the start of the waterhammer pressure wave record when the pipe is probably only slightly defective, the primary wave is the dominant feature in the wave spectrum.

(2) There is also a peak in the spectrum associated with a low frequency rigid column wave, probably arising from vapour pocket formation or small air pockets. This wave is not distinguishable in the early records, but shows up clearly in the power spectrum. This wave has an initial period of approximately 8 times that of the waterhammer wave. This wave proves to be important, contributing to the failure of the forcemain.

(3) There is a significant deterioration of the primary waterhammer wave on the 6th record (corresponding to the 6th pump stoppage). At this time the primary waterhammer wave suddenly reduced and the wave energy spread over a greater frequency band. There is also an increase in both the peak and the frequency of the rigid column wave. This wave becomes the dominant feature in the spectrum at this stage.

The explanation offered is that a crack or small break has occurred in the line. This break is not large enough to show up on the ground surface, but it does have an effect on the primary waterhammer wave. The waves show an upward frequency shift. This is probably the result of reflection of part of the wave at the crack, and the introduction of air into the forcemain.

(4) The rigid column wave showed a dramatic frequency shift in the last 2 records before the ultimate collapse of the main, the wave period decreasing to approximately 9 secs from 33 secs. initially. The peak of the wave in the power spectrum increased to a value 4.5 times that of the initial record.

(5) The area under the power spectrum in any frequency band represents the proportionate amount of power available in that band. Evidently a large amount of energy built up in a narrow frequency band centred on 0.11 hertz(9sec. period). This energy resulted in the ultimate failure of the forcemain.

(6) Once a small failure occurs in a forcemain subject to column separation, there is a strong possibility that the crack will inject air into the vapour pocket. With continued use the incipient condition will deteriorate letting in more air. This alters the tuning of the low frequency wave. The probability is high that the residual primary wave will superimpose with the upwardly tuning low frequency wave to produce high pressures of short duration. Such pressures could result in complete collapse of the rapidly deteriorating pipeline.

(7) On-line power spectral analysis offers an interesting opportunity to monitor important pumping pipelines and provide advance warning of potential pipeline collapse.

6. RECOMMENDATIONS FOR FURTHER STUDY

This problem should be subject to further study, specifically in the following areas:

(1) Pressure waves in the pipeline should be recorded and analysed when the line is repaired. This would provide a better "zero base" to inspect the observed or future changes in frequency.

(2) Attempt to refine the power spectral estimates to get a better representation of the shift in significant frequencies.

This would include:

- (a) better editing of the observed pressures.
- (b) filtering and selecting appropriate data windows and checking for aliasing.
- (c) investigating other subprogrammes for calculating power spectra, (eg. BMDO2T).

(3) Make use of improved spectral estimates to attempt to mathematically link the change in frequency in the power spectrum to the waves present in the pipe. It appears that one can ascertain qualitatively from the power spectrum when an incipient pipe break has occurred. Further attempts should be made on a quantitative basis to relate the shift in frequency to the actual location of the break.

(4) Extend the spectral analysis into the examination of the efficiency of the pressure vessels currently in use in the pipeline.

REFERENCES

1. Protection Against Waterhammer in Pump Discharge Lines — Kassem, Atef, M. Masters Thesis, McMaster University, March, 1976.

2. Fluid Mechanics — Streeter, Victor L. McGraw-Hill, 1951.

3. Mechanics of Fluids — Massy, B.S. Van Nostrand Reinhold, 1968.

4. Waterhammer Analysis — Parmakian, John Prentice-Hall, 1955.

5. Lecture Notes Taken From Graduate Studies, Department of Civil Engineering, McMaster University — Dr. W. James

6. Introduction to Wave Spectrum Analysis — J. W. Kamphuis Queens University

7. Measurement of Power Spectra — R. B. Blackman and J. W. Tukey

APPENDIX I

SAMPLE OF PRESSURE RECORDINGS

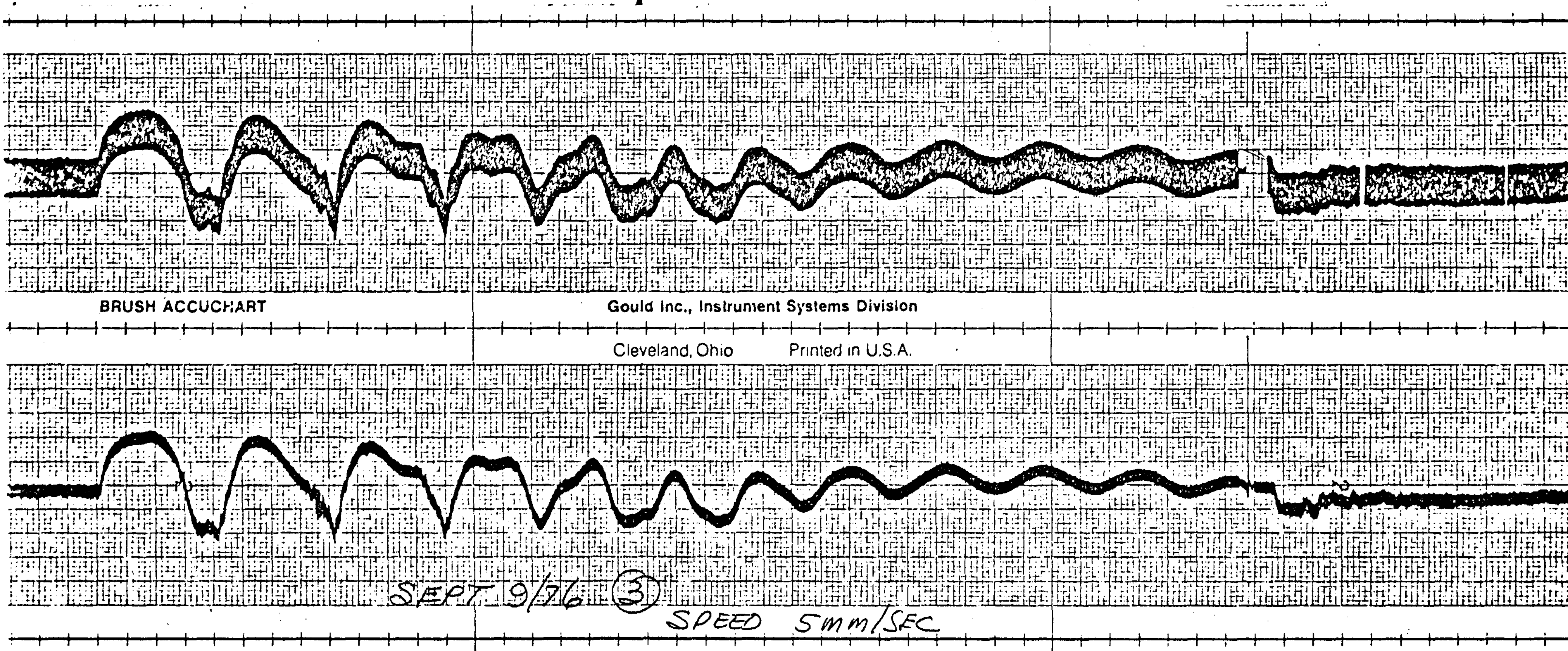

PRESSURE RECORD No. 2

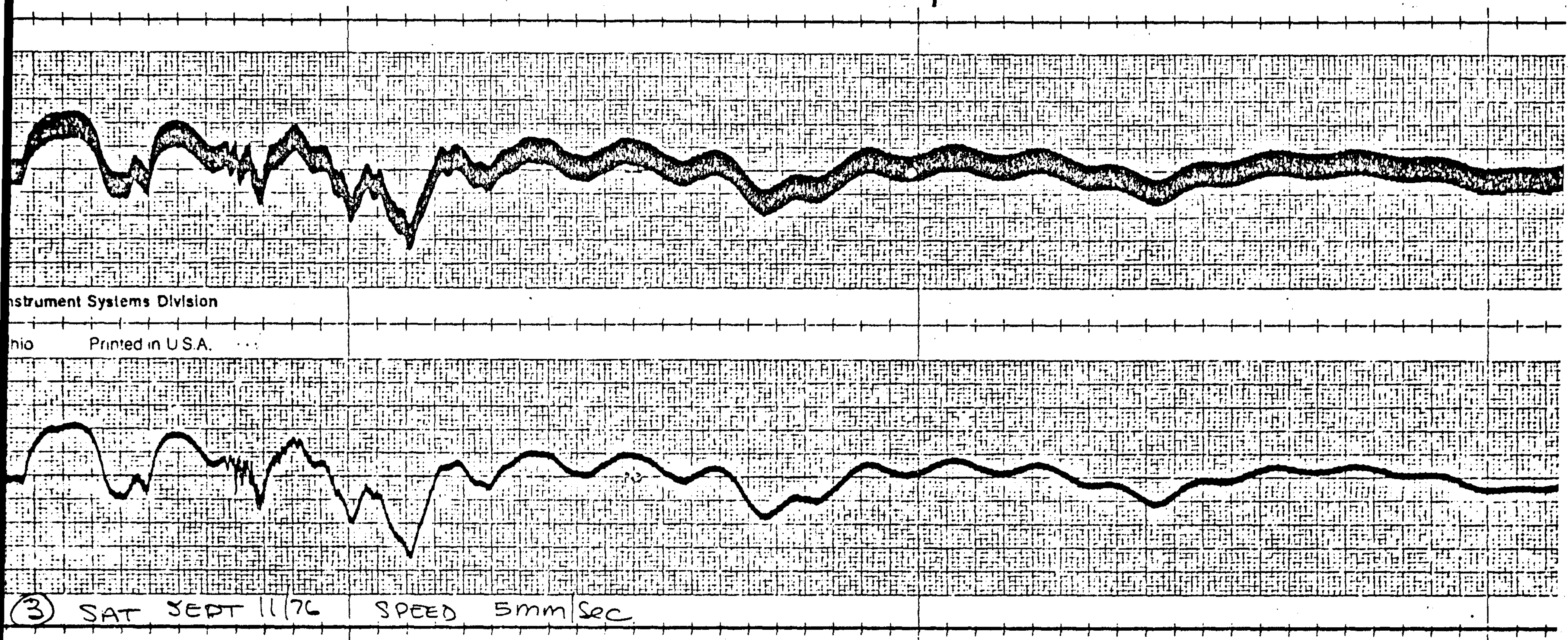

PRESSURE RECORD No. 10

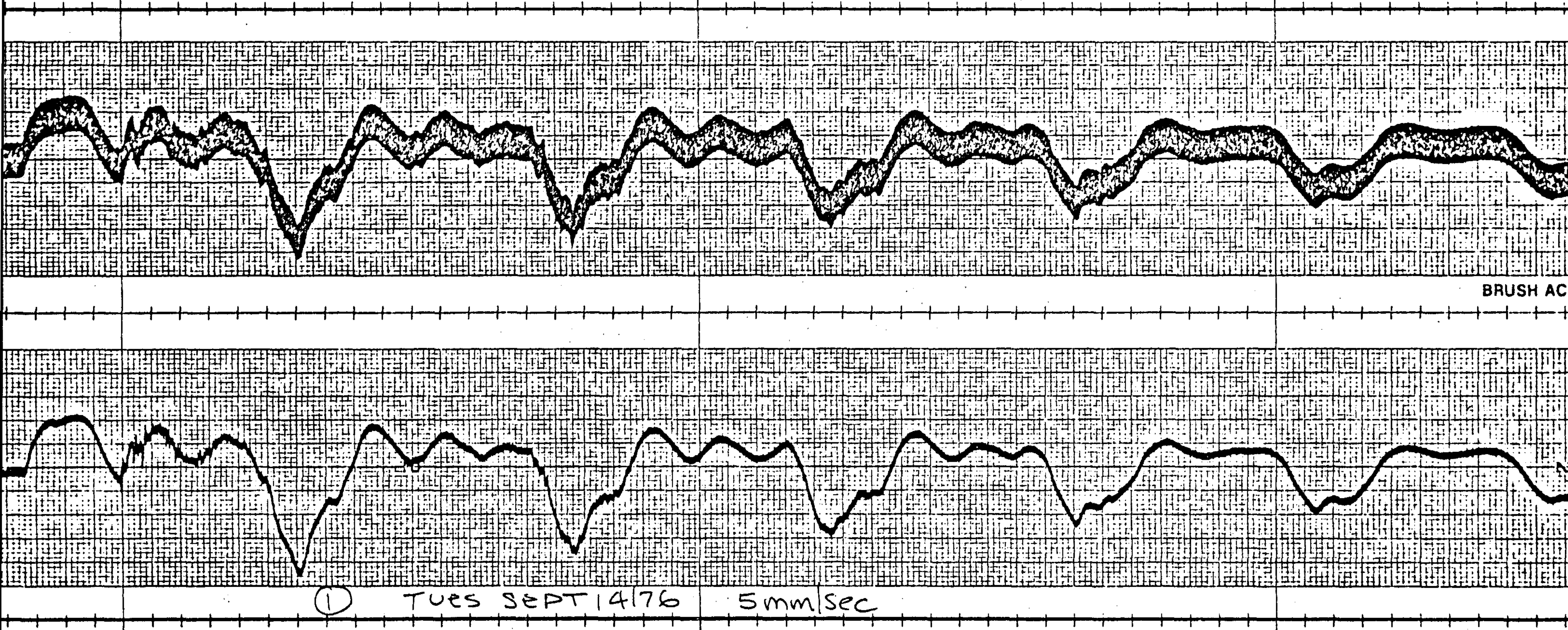

PRESSURE RECORD No. 18

APPENDIX II

POWER SPECTRA FOR EACH PRESSURE RECORDING

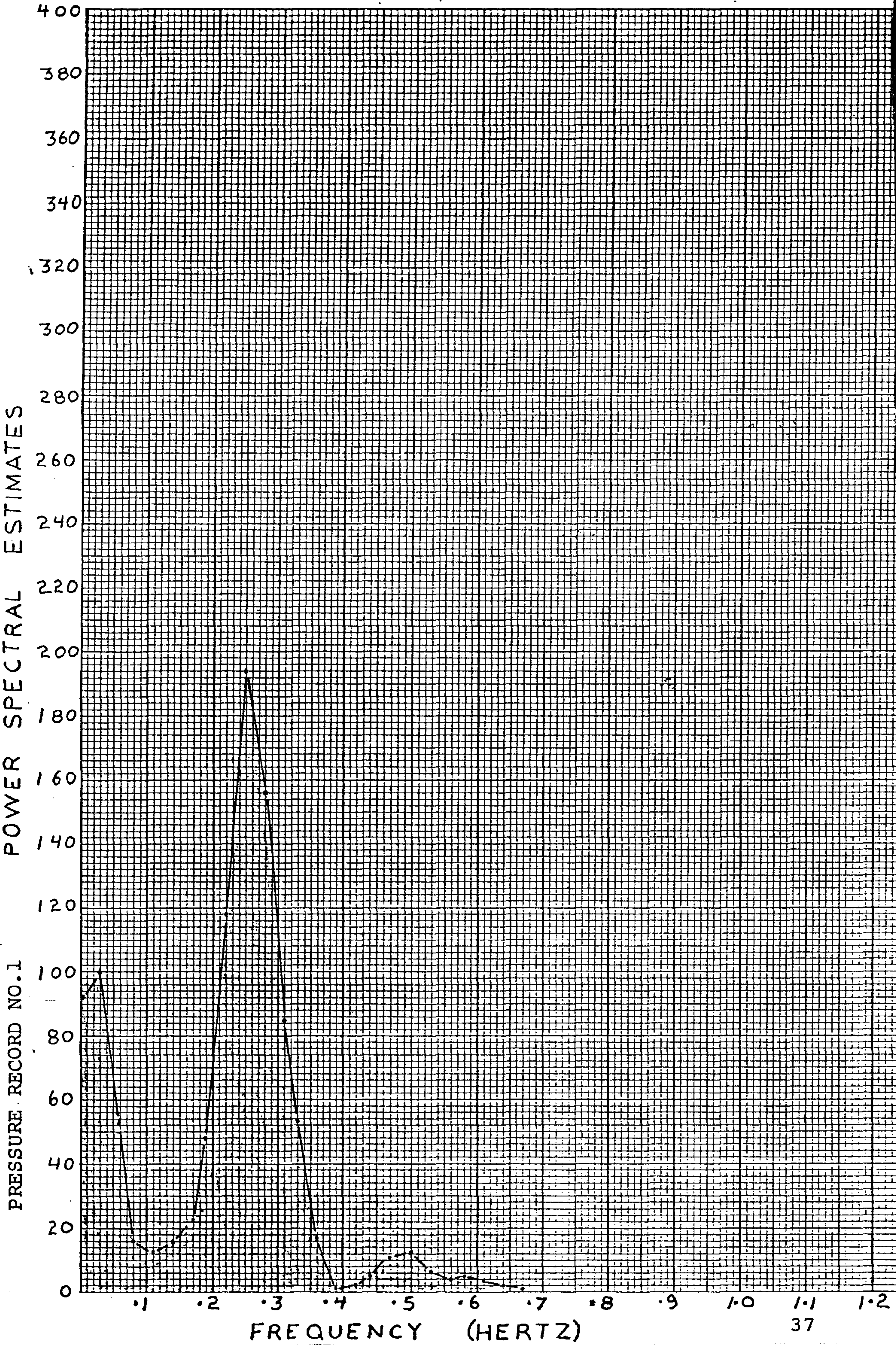

400
380
360
340
320
300
280
260
240
220
200
180
160
140
120
100
80
60
40
20
0
POWER SPECTRAL ESTIMATES
PRESSURE RECORD NO.1
·1
·2
·3
·4
·5
·6
·7
·8
·9
1·0
1·1
1·2
FREQUENCY (HERTZ)

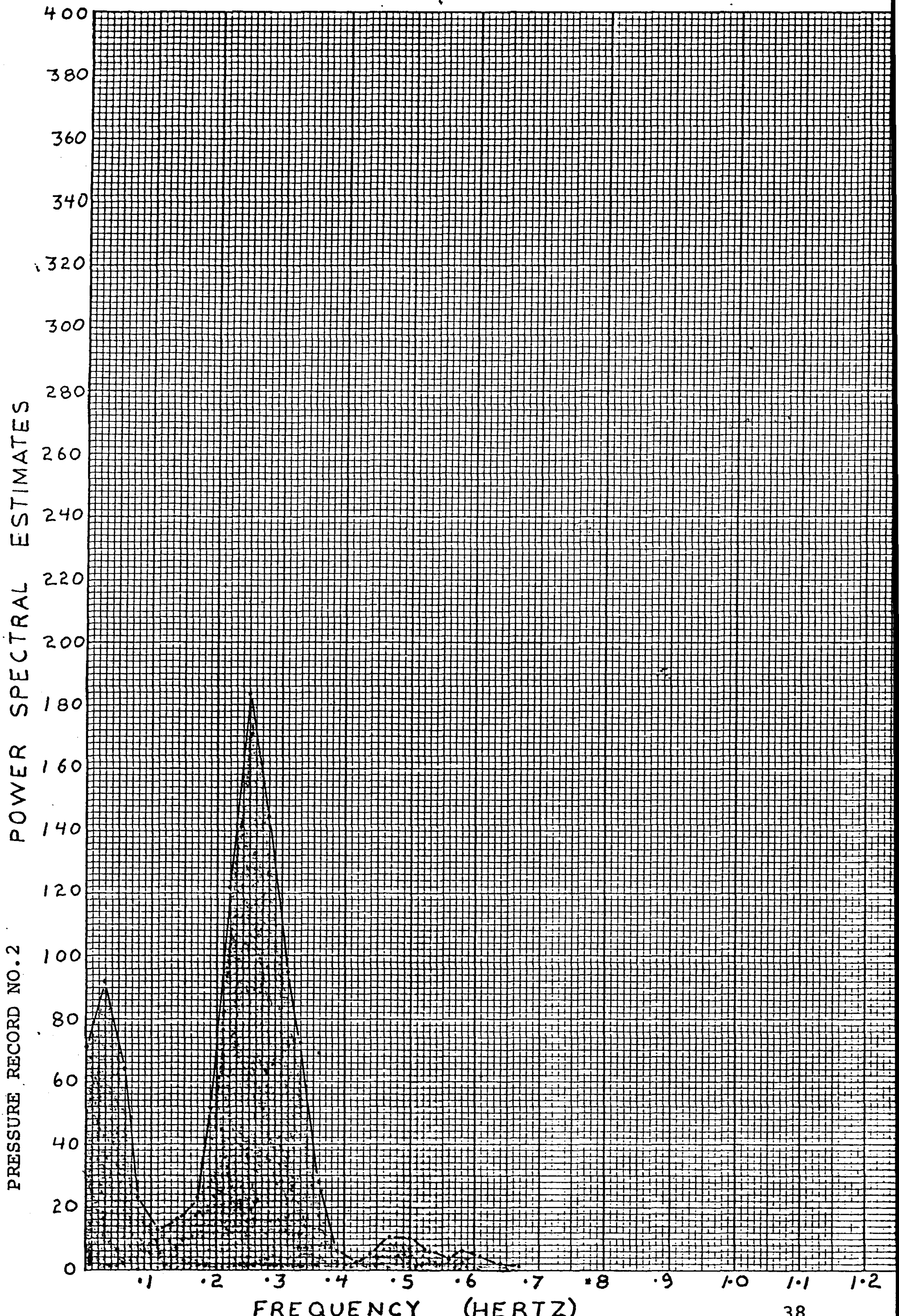

400
380
360
340
320
300
280
260
240
220
200
180
160
140
120
100
80
60
40
20
0
·1
·2
·3
·4
·5
·6
·7
·8
·9
1·0
1·1
1·2
FREQUENCY (HERTZ)
POWER SPECTRAL ESTIMATES
PRESSURE RECORD NO.2

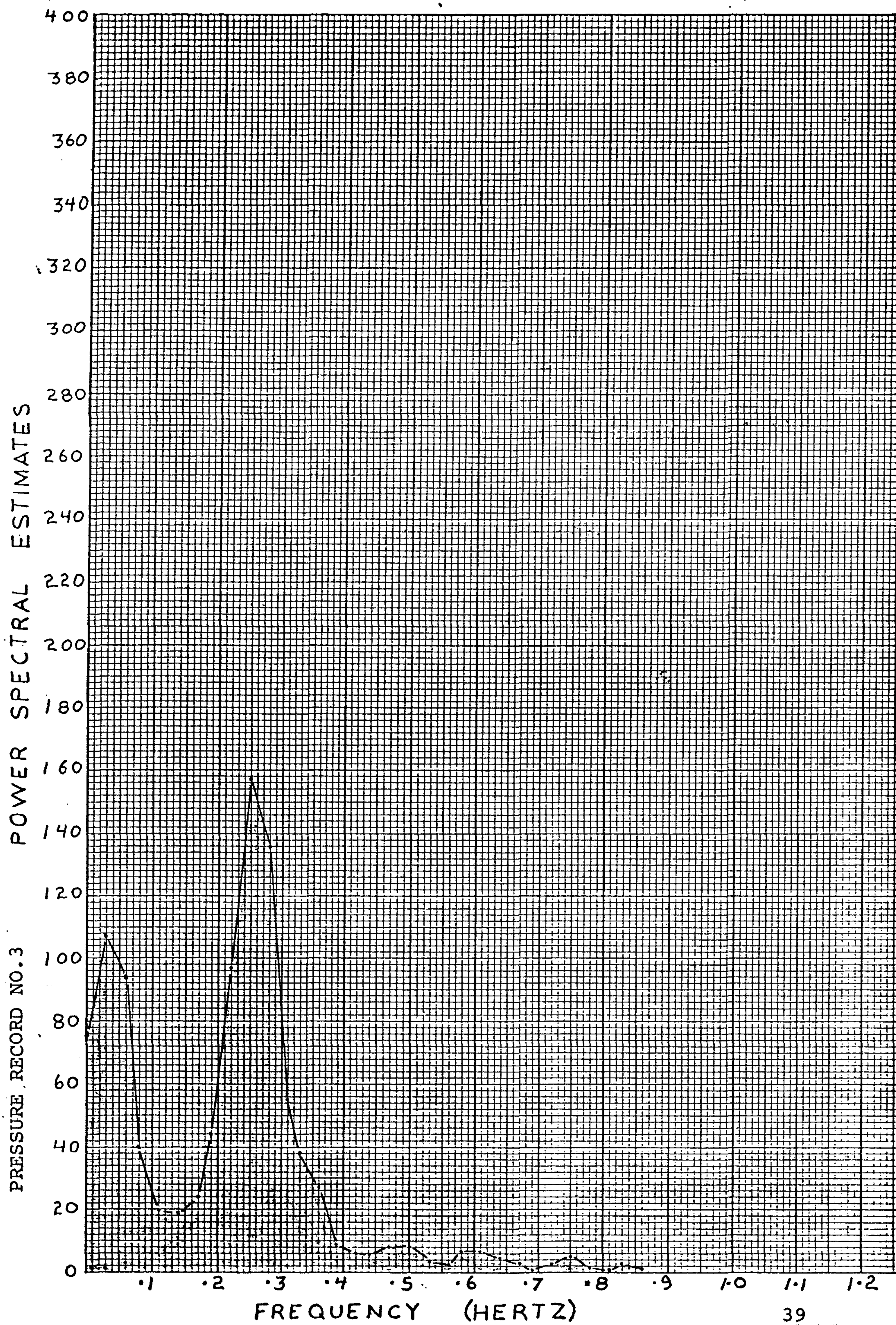

400
380
360
340
320
300
280
260
240
220
200
180
160
140
120
100
80
60
40
20
0
POWER SPECTRAL ESTIMATES
PRESSURE RECORD NO.3
·1
·2
·3
·4
·5
·6
·7
·8
·9
1·0
1·1
1·2
FREQUENCY (HERTZ)

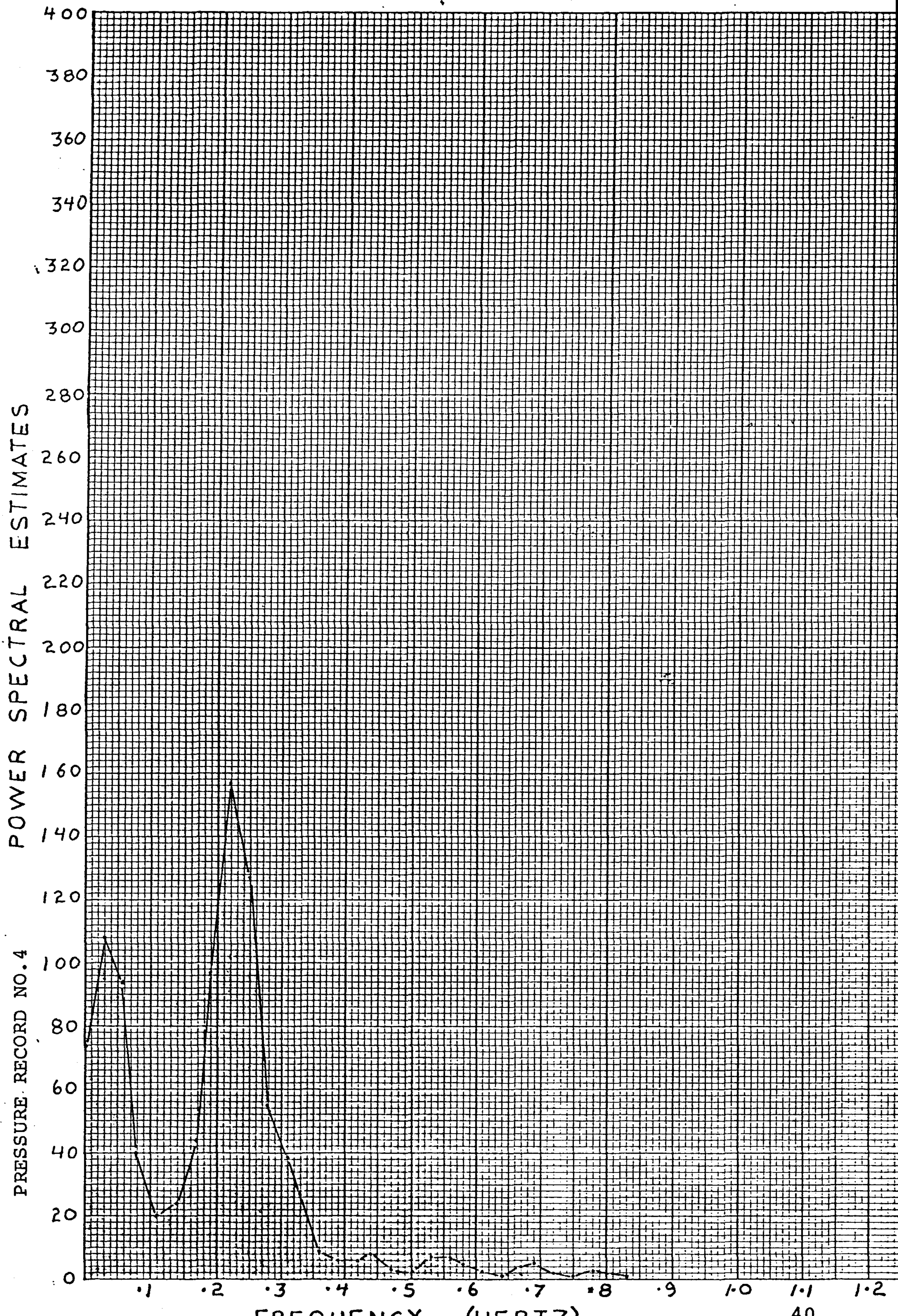
400
380
360
340
320
300
280
260
240
220
200
180
160
140
120
100
80
60
40
20
0
POWER SPECTRAL ESTIMATES
PRESSURE RECORD NO.4
·1
·2
·3
·4
·5
·6
·7
·8
·9
1·0
1·1
1·2
FREQUENCY (HERTZ)

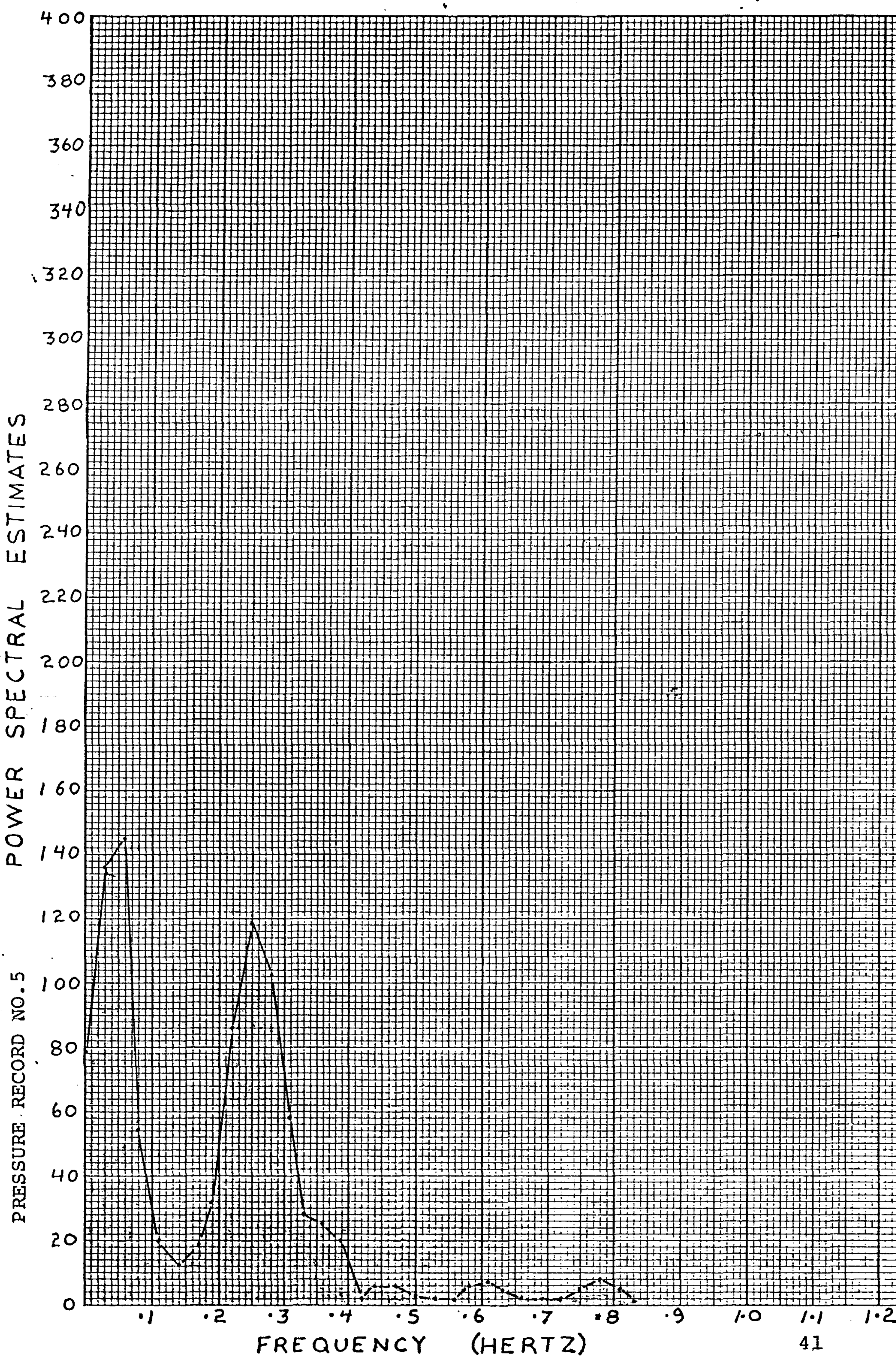

POWER SPECTRAL ESTIMATES
PRESSURE RECORD NO.5
400
380
360
340
320
300
280
260
240
220
200
180
160
140
120
100
80
60
40
20
0
·1
·2
·3
·4
·5
·6
·7
·8
·9
1·0
1·1
1·2
FREQUENCY (HERTZ)

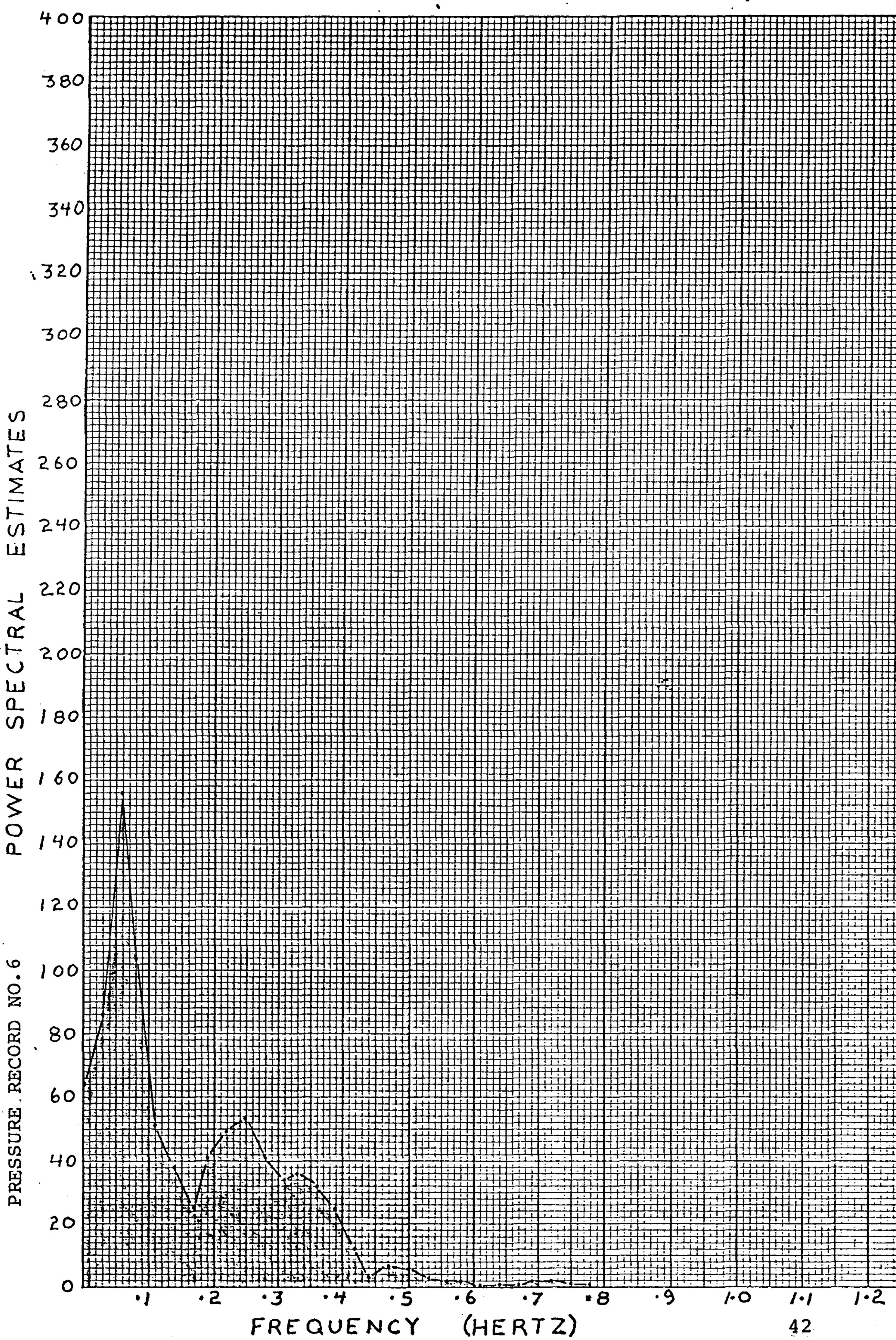
POWER SPECTRAL ESTIMATES
PRESSURE RECORD NO. 6
400
380
360
340
320
300
280
260
240
220
200
180
160
140
120
100
80
60
40
20
0
·1
·2
·3
·4
·5
·6
·7
·8
·9
1·0
1·1
1·2
FREQUENCY (HERTZ)

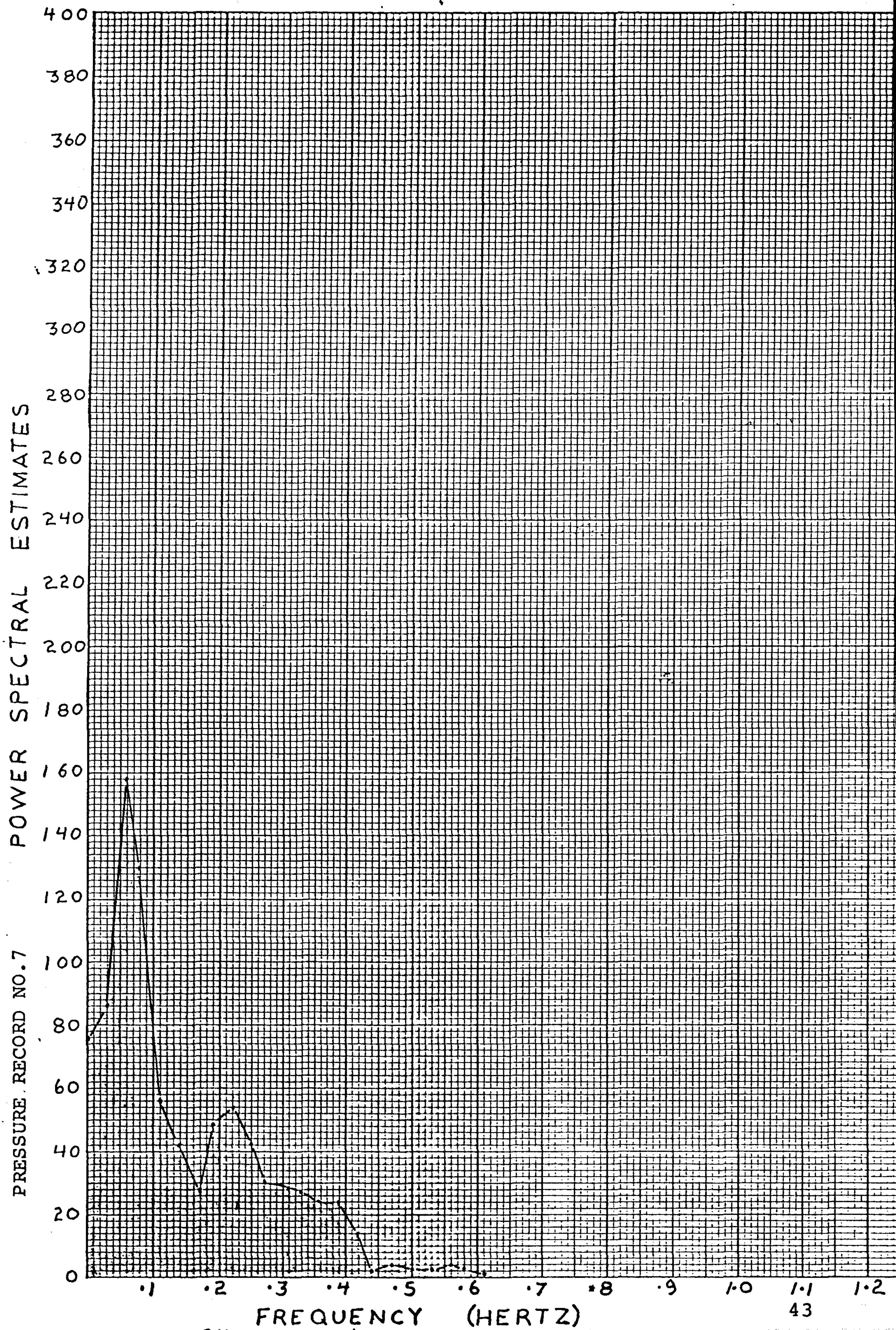

POWER SPECTRAL ESTIMATES
PRESSURE RECORD NO.7
400
380
360
340
320
300
280
260
240
220
200
180
160
140
120
100
80
60
40
20
0
·1
·2
·3
·4
·5
·6
·7
·8
·9
1·0
1·1
1·2
FREQUENCY (HERTZ)

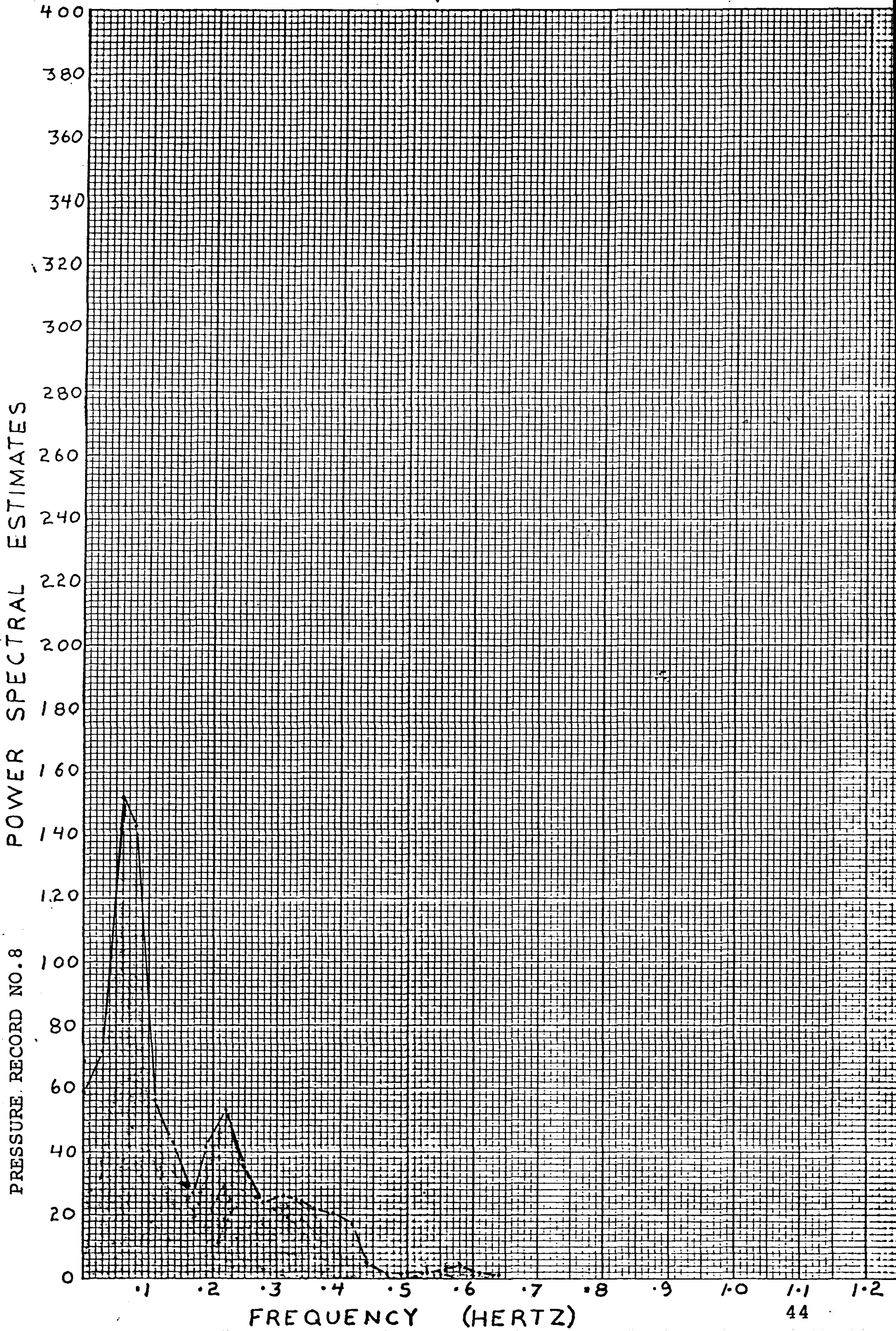
400
380
360
340
320
300
280
260
240
220
200
180
160
140
120
100
80
60
40
20
0
POWER SPECTRAL ESTIMATES
PRESSURE RECORD NO.8
·1
·2
·3
·4
·5
·6
·7
·8
·9
1·0
1·1
1·2
FREQUENCY (HERTZ)

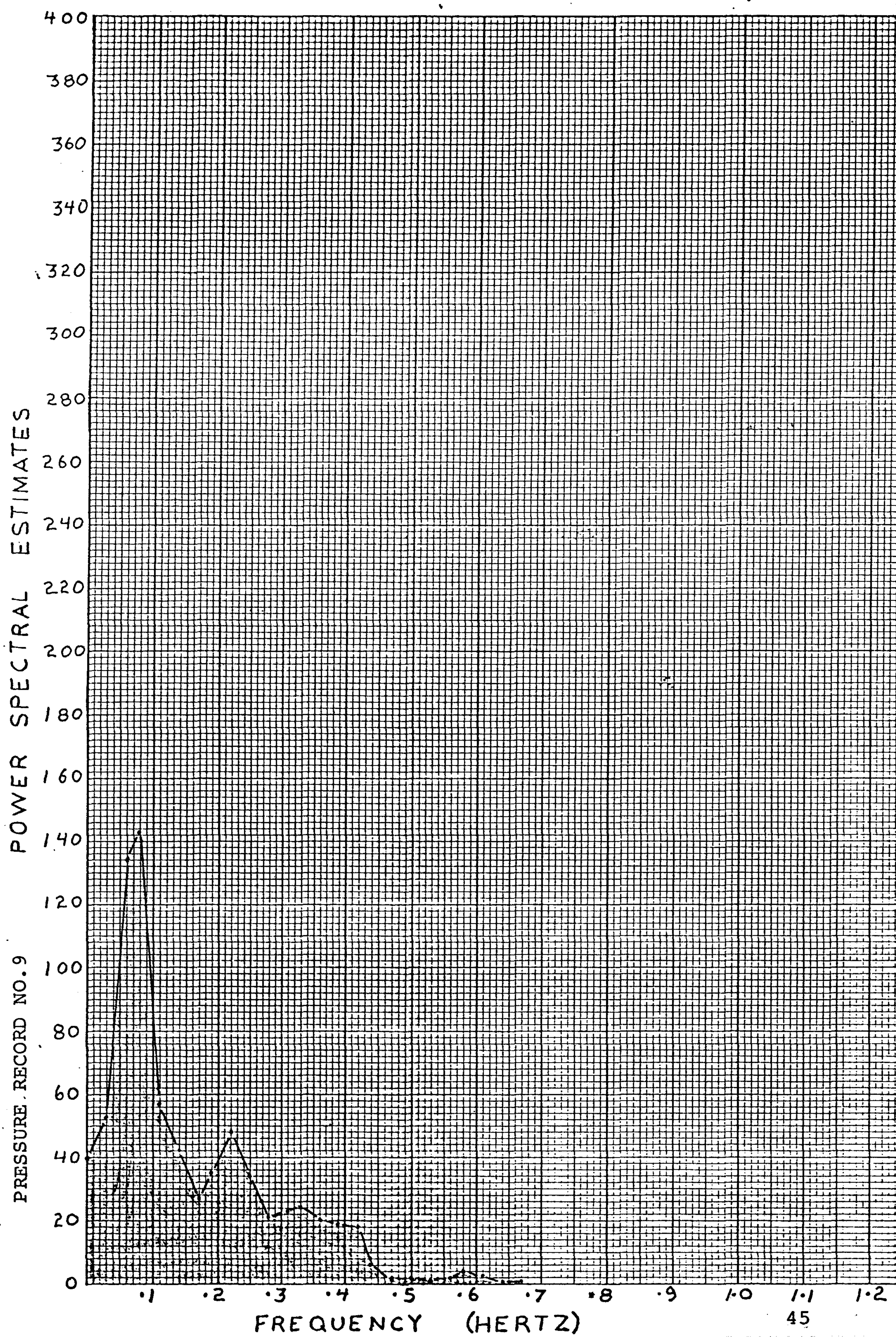
POWER SPECTRAL ESTIMATES
PRESSURE RECORD NO.9
400
380
360
340
320
300
280
260
240
220
200
180
160
140
120
100
80
60
40
20
0
·1
·2
·3
·4
·5
·6
·7
·8
·9
1·0
1·1
1·2
FREQUENCY (HERTZ)

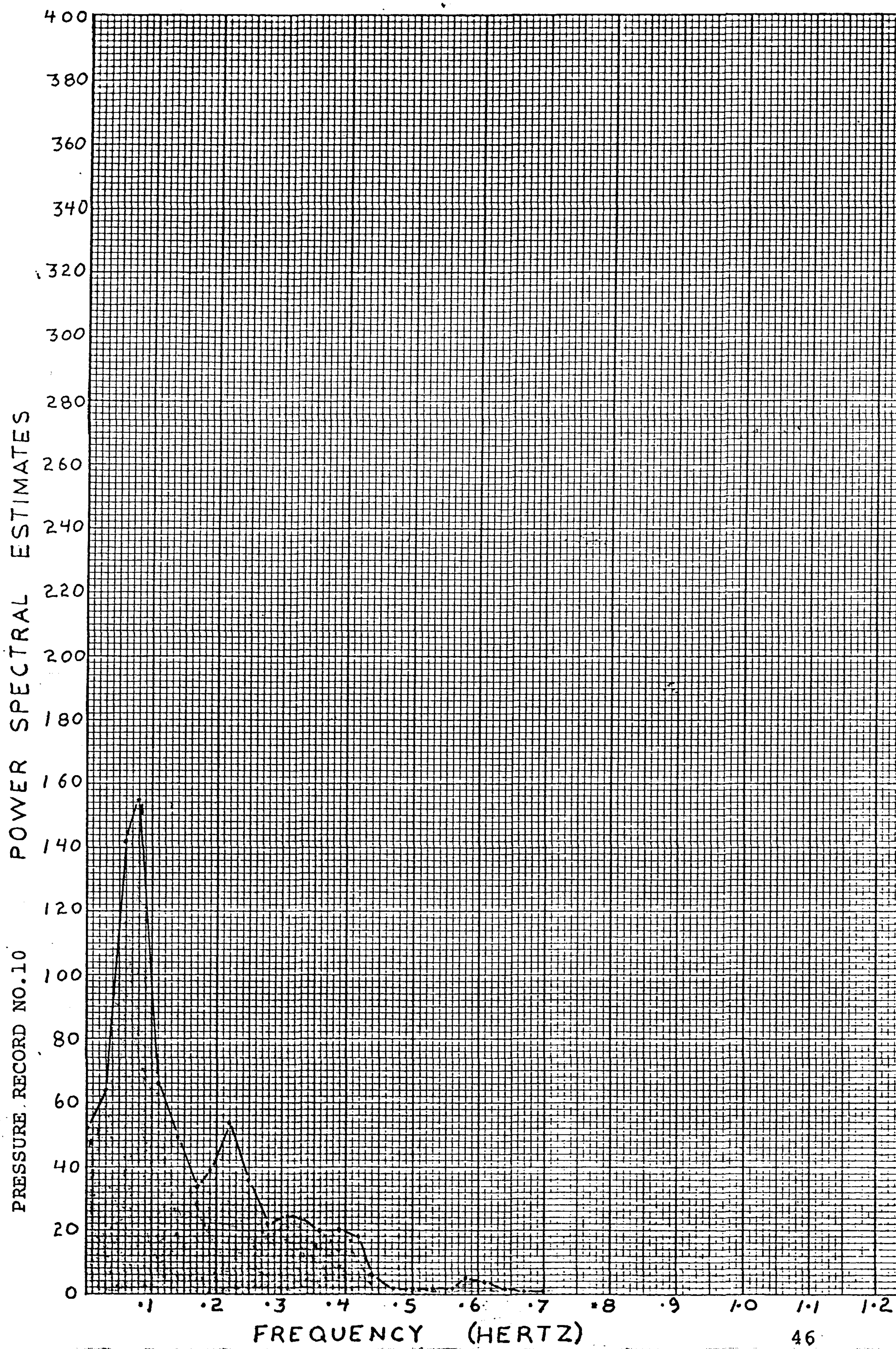

400
380
360
340
320
300
280
260
240
220
200
180
160
140
120
100
80
60
40
20
0
POWER SPECTRAL ESTIMATES
PRESSURE RECORD NO.10
·1
·2
·3
·4
·5
·6
·7
·8
·9
1·0
1·1
1·2
FREQUENCY (HERTZ)

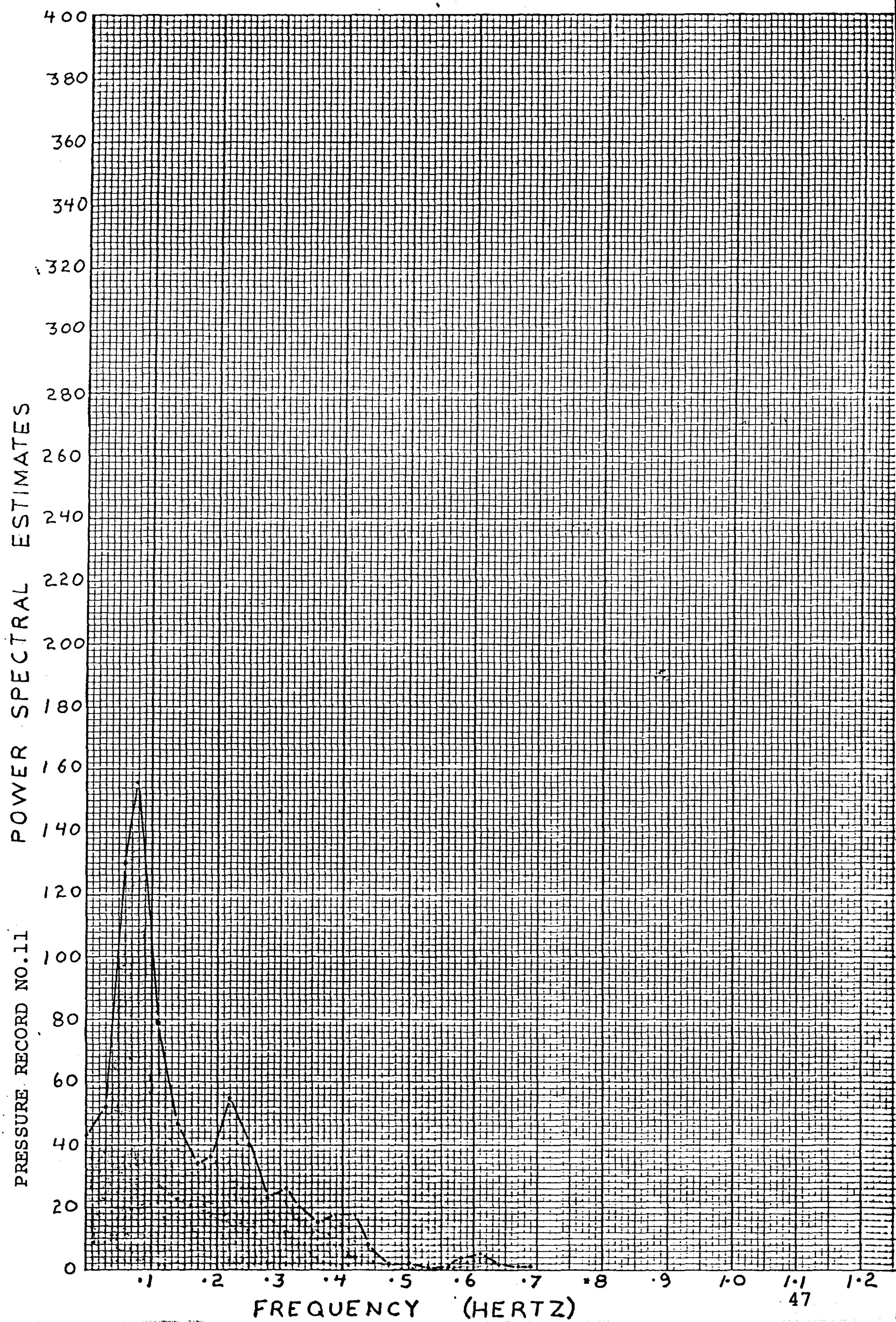
POWER SPECTRAL ESTIMATES
PRESSURE RECORD NO.11
400
380
360
340
320
300
280
260
240
220
200
180
160
140
120
100
80
60
40
20
0
·1
·2
·3
·4
·5
·6
·7
·8
·9
1·0
1·1
1·2
FREQUENCY (HERTZ)

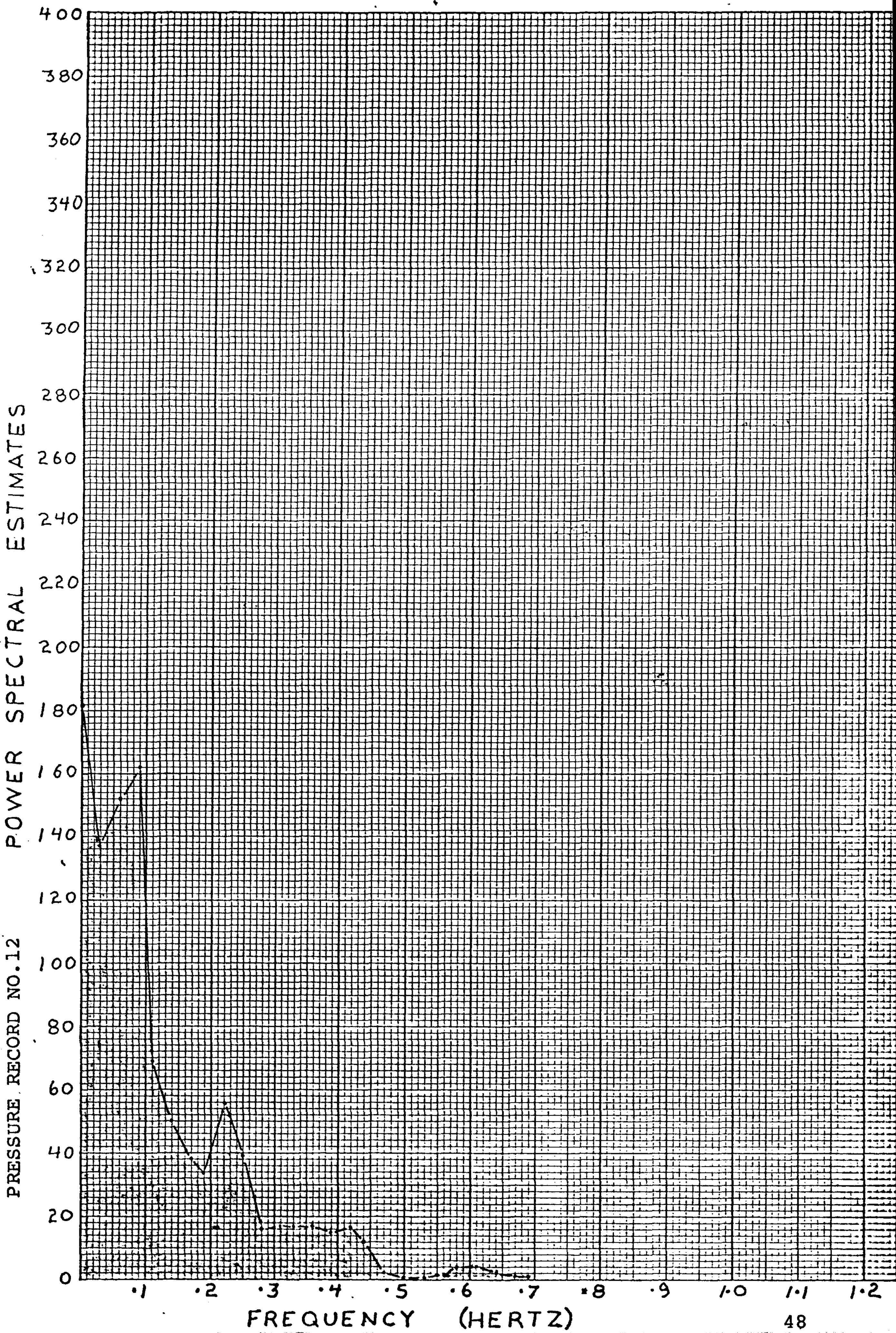

PRESSURE RECORD NO. 12
POWER SPECTRAL ESTIMATES
400
380
360
340
320
300
280
260
240
220
200
180
160
140
120
100
80
60
40
20
0
·1
·2
·3
·4
·5
·6
·7
·8
·9
1·0
1·1
1·2
FREQUENCY (HERTZ)

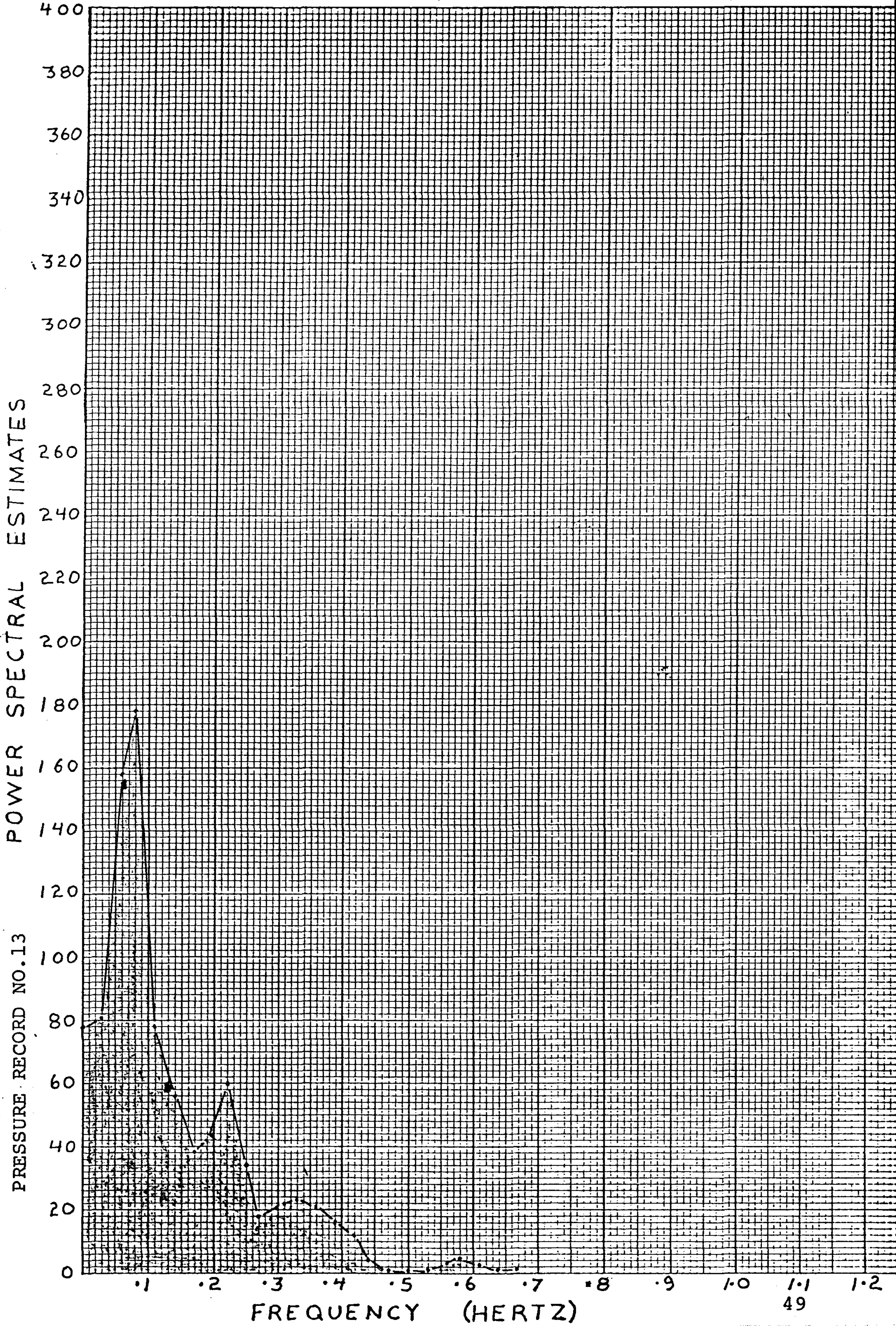

400
380
360
340
320
300
280
260
240
220
200
180
160
140
120
100
80
60
40
20
0
POWER SPECTRAL ESTIMATES
PRESSURE RECORD NO.13
·1
·2
·3
·4
·5
·6
·7
·8
·9
1·0
1·1
1·2
FREQUENCY (HERTZ)

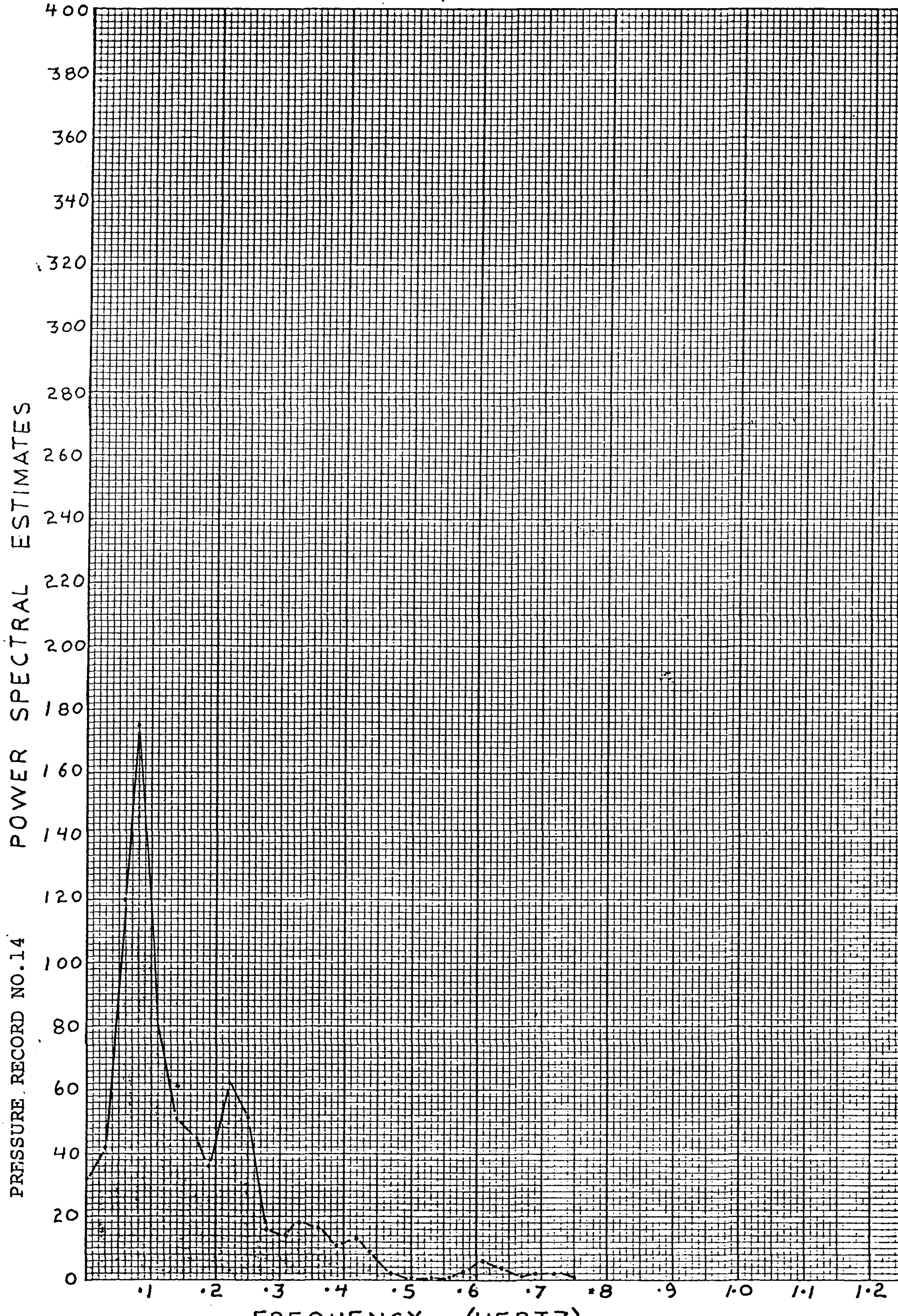
PRESSURE RECORD NO.14
POWER SPECTRAL ESTIMATES
400
380
360
340
320
300
280
260
240
220
200
180
160
140
120
100
80
60
40
20
0
·1
·2
·3
·4
·5
·6
·7
·8
·9
1·0
1·1
1·2
FREQUENCY (HERTZ)

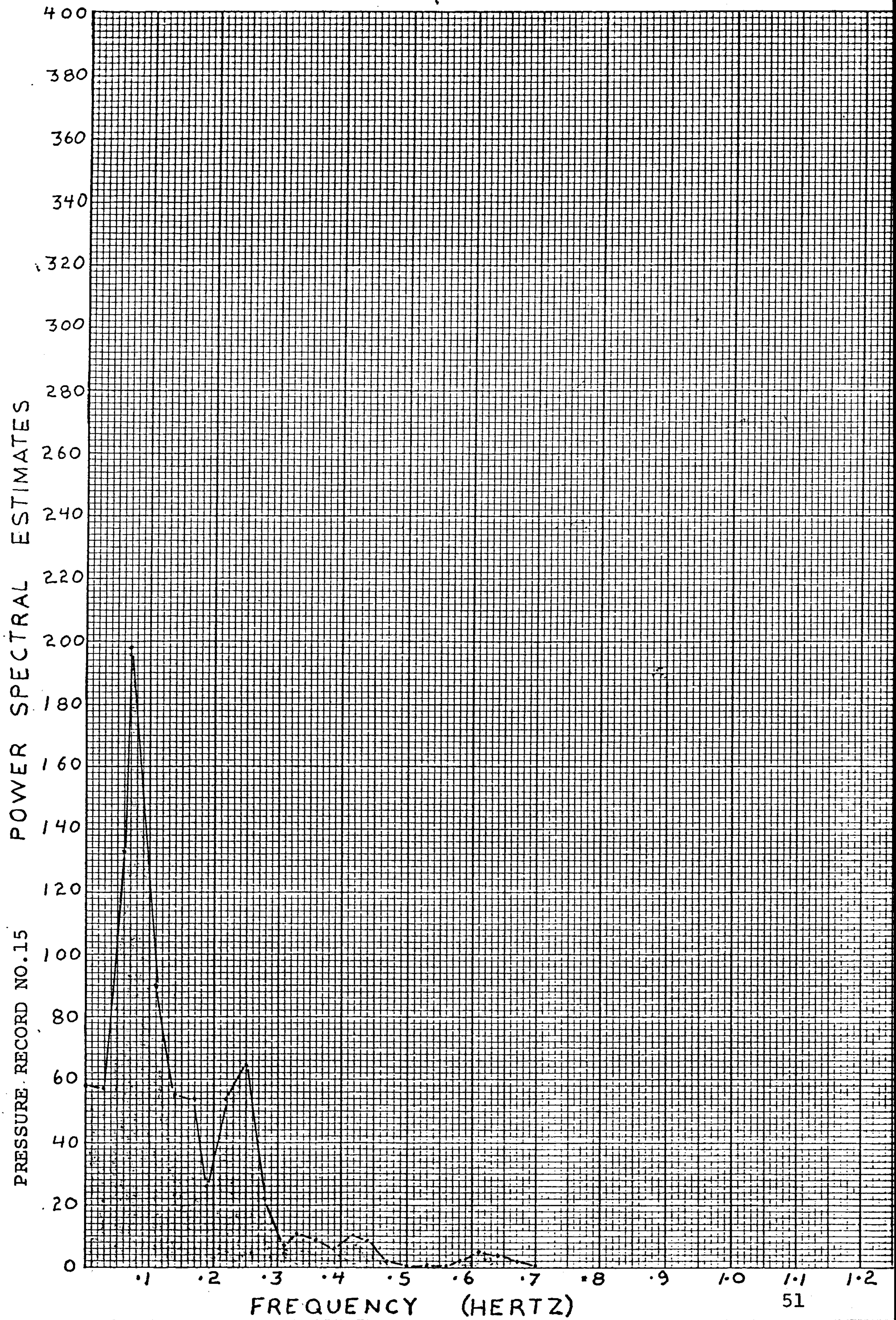
PRESSURE RECORD NO.15
POWER SPECTRAL ESTIMATES
400
380
360
340
320
300
280
260
240
220
200
180
160
140
120
100
80
60
40
20
0
·1
·2
·3
·4
·5
·6
·7
·8
·9
1·0
1·1
1·2
FREQUENCY (HERTZ)

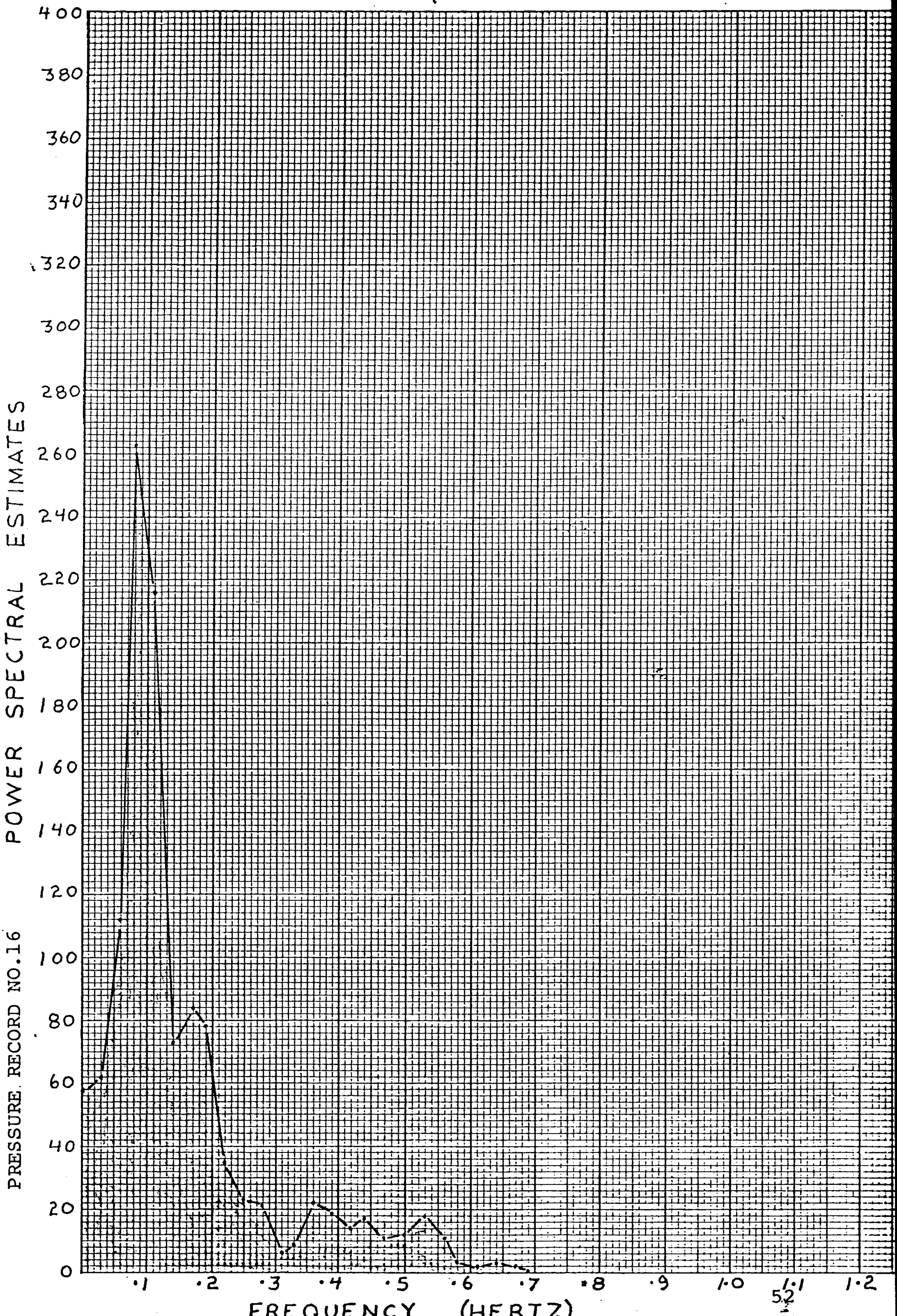

POWER SPECTRAL ESTIMATES
PRESSURE RECORD NO.16
400
380
360
340
320
300
280
260
240
220
200
180
160
140
120
100
80
60
40
20
0
·1
·2
·3
·4
·5
·6
·7
·8
·9
1·0
1·1
1·2
FREQUENCY (HERTZ)

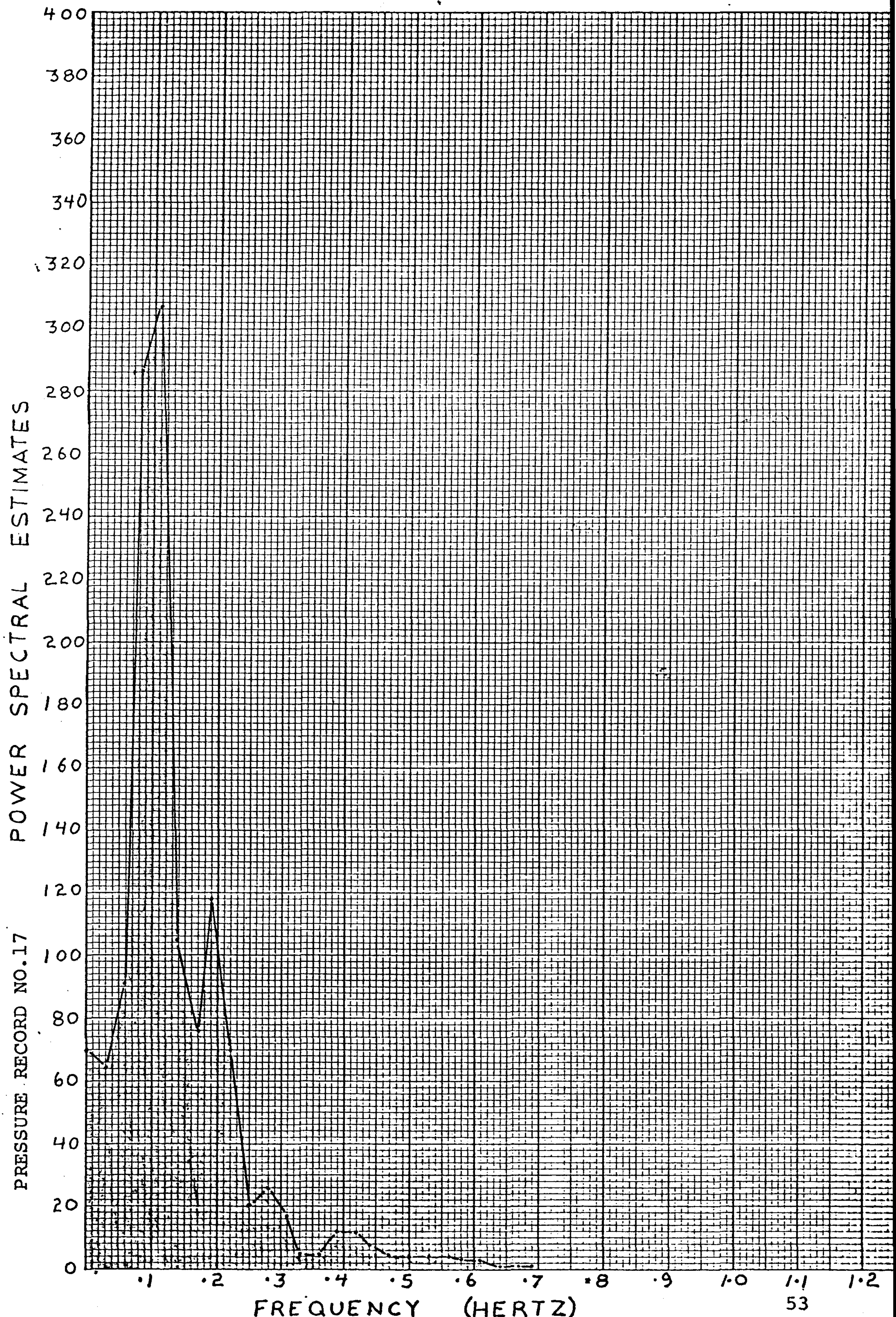
POWER SPECTRAL ESTIMATES
PRESSURE RECORD NO.17
400
380
360
340
320
300
280
260
240
220
200
180
160
140
120
100
80
60
40
20
0
·1
·2
·3
·4
·5
·6
·7
·8
·9
1·0
1·1
1·2
FREQUENCY (HERTZ)

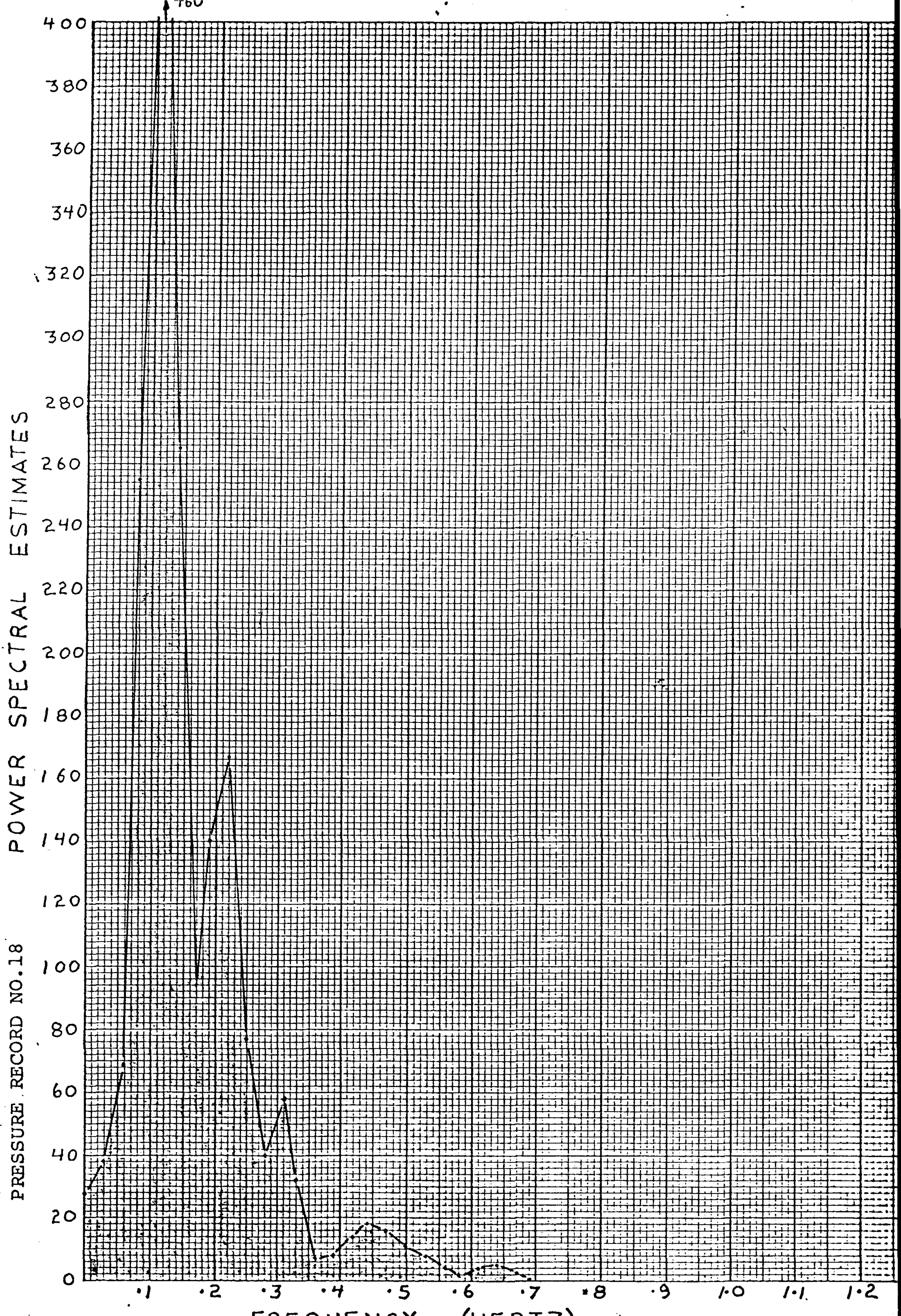

460
400
380
360
340
320
300
280
260
240
220
200
180
160
140
120
100
80
60
40
20
0
POWER SPECTRAL ESTIMATES
PRESSURE RECORD NO.18
·1
·2
·3
·4
·5
·6
·7
·8
·9
1·0
1·1
1·2
FREQUENCY (HERTZ)

APPENDIX III

COMPUTER PROGRAM LISTING

```
 MMU  MCMASTER-SCOPE 3.4.4RELEASE420 05/03/77
18.11.20.HRJHONR   FROM
18.11.20.IP   00000384 WORDS - FILE INPUT  , DC 00
18.11.20.HRJH.
18.11.20.                                   HENNESSY R
18.11.21.FTN,EL=A,R=3.
18.11.22./ 44000B    CM STORAGE USED
18.11.22./T      .317 CP SECONDS COMPILATION TIME
18.11.22.ATTACH,TAPE7,AHAMMERDATA,ID=HRJH.
18.11.23.PF CYCLE NO. = 002
18.11.23.ATTACH,IMSLIB.
18.11.23.PFN IS
18.11.23.IMSLIB
18.11.23.PF CYCLE NO. = 053
18.11.23.LDSET(LIB=IMSLIB)
18.11.23.LGO(PL=1600)
18.11.31.      STOP
18.11.31.        5626 WORDS NEVER USED
18.11.31.       3.552 CP SECONDS EXECUTION TIME
18.11.31.OP   00002048 WORDS - FILE OUTPUT  , DC 40
18.11.31.MS      3584   WORDS   (    14336 MAX USED)
18.11.31.CPA          5.555 SEC.          2.500 ADJ.
18.11.31.IO           3.324 SEC.           .332 ADJ.
18.11.31.CM         154.496 KWS.          1.616 ADJ.
18.11.31.SS                               4.448
18.11.31.PP           7.168 SEC.      DATE 06/15/77
18.11.31.COMPUTING COST AT $416/HOUR            $.74
18.11.31.ESTIMATED UNIT RECORD COST             $.25
18.11.31.ESTIMATED TOTAL COST                  $1.00
18.11.31.EJ  END OF JOB, **

***********          HRJHONR  //// END OF LIST ////
***********          HRJHONR  //// END OF LIST ////
```

```
      PROGRAM SPEC(INPUT,OUTPUT,TAPE5=INPUT,TAPE6=OUTPUT,TAPE7)
STATEMENT IS NOT DEFINED IN ANSI
      DIMENSIONXX(5000),IND(6),XIND(2),XYMV(6),ACV(183),FREQ(91),PS(91)
        DIMENSICN X(335)
        REWIND 7
 10     FORMAT(≠-≠,≠MEAN  AND  VARIENCE≠)
 11     FORMAT(≠1≠,≠FREQUENCY≠)
 12   FORMAT(≠1≠,≠TOTAL DATA PTS,START READ,END READ≠)
 13     FORMAT(≠1≠,≠                 POWER SPECTRA≠)
100     FORMAT(5X,F4.0)
200     FORMAT(F4.2)
300     FORMAT(I3)
400     FORMAT(F12.2)
500      FCRMAT(3I10)
 600    FCRMAT(≠ ≠,12X,F12.2)
700     FORMAT(5X,F5.0)
      DO 2 I=1,6
      READ(5,300)IND(I)
  2     CONTINUE
      DO 3 I=1,2
        READ(5,200)XIND(I)
  3   CONTINUE
      READ(5,500)J,L,M
       NPTS=M-L
      READ(7,100)(XX(I),I=1,J)
      DO 4 I=1,NPTS
      X(I)=XX(L+I)
  4   CONTINUE
      DO 1 I=1,NPTS
      IF(X(I).GT.5000)X(I)=-(10000-X(I))
 1      CONTINUE
      DO 5 I=1,NPTS
      X(I)=-(X(I))
      IF(X(I).GE.100)  X(I)=0
      IF(X(I).LE.-100)  X(I)=0
      WRITE(6,700)X(I)
  5     CONTINUE
      CALL FTFREQ(X,IND,XIND,XYMV,ACV,FREQ,PS,XCOV,XSPECT,AMPHAS,
     *XFER,COHER,IER)
        WRITE(6,12)
        WRITE(6,500)J,L,M
      WRITE(6,10)
      WRITE(6,400)XYMV
      WRITE(6,11)
      WRITE(6,400)FREQ
      WRITE(6,13)
      WRITE(6,600)PS
      STCP
      END
```

INTS--

3B	INPUT=	43B	OUTPUT=	153B	SPEC	3B	TAPE5=
43B	TAPE6=	103B	TAPE7=				

57

APPENDIX IV

POWER SPECTRA WITHIN SELECTED PRESSURE RECORDS

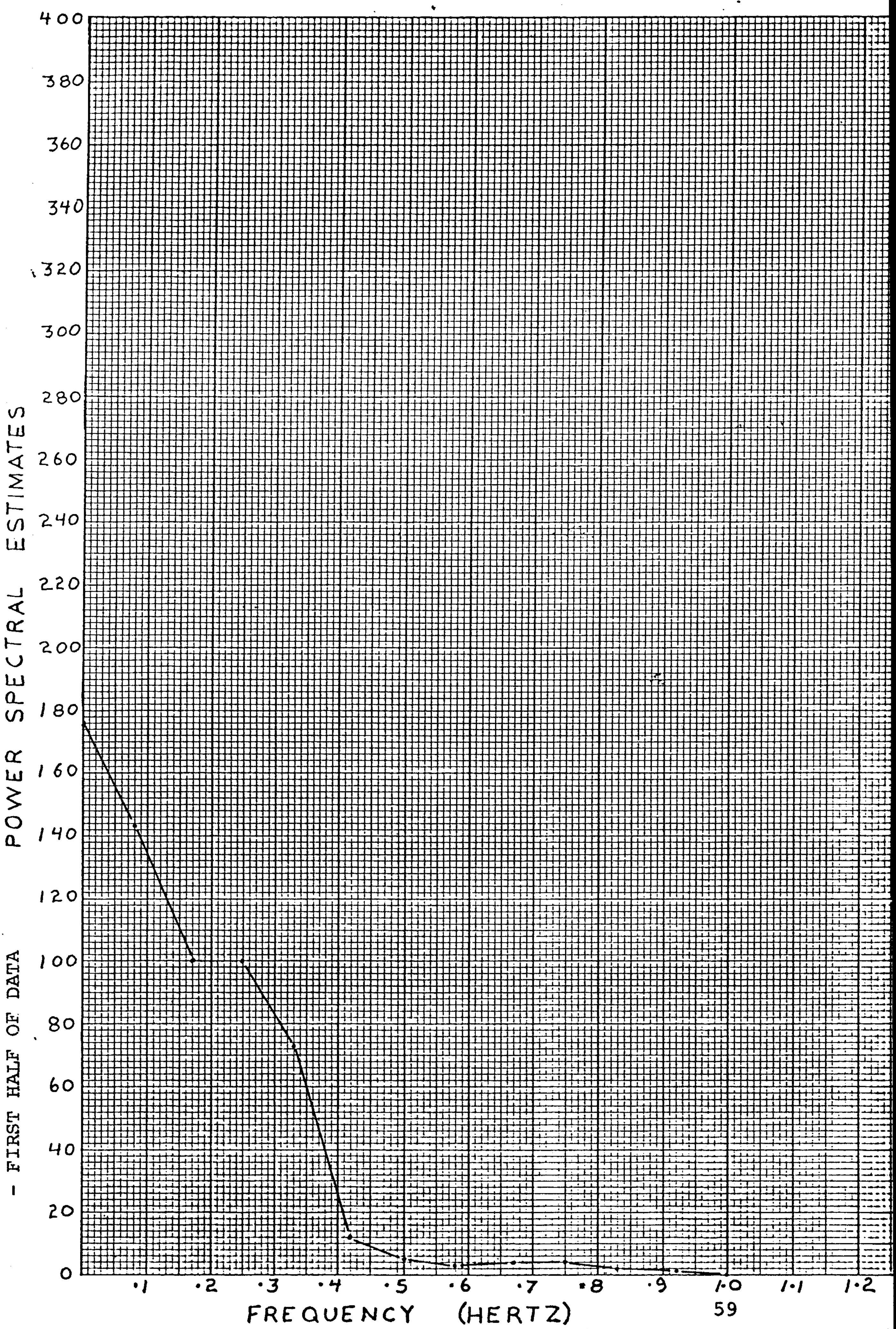

PRESSURE RECORD NO. 6
- FIRST HALF OF DATA

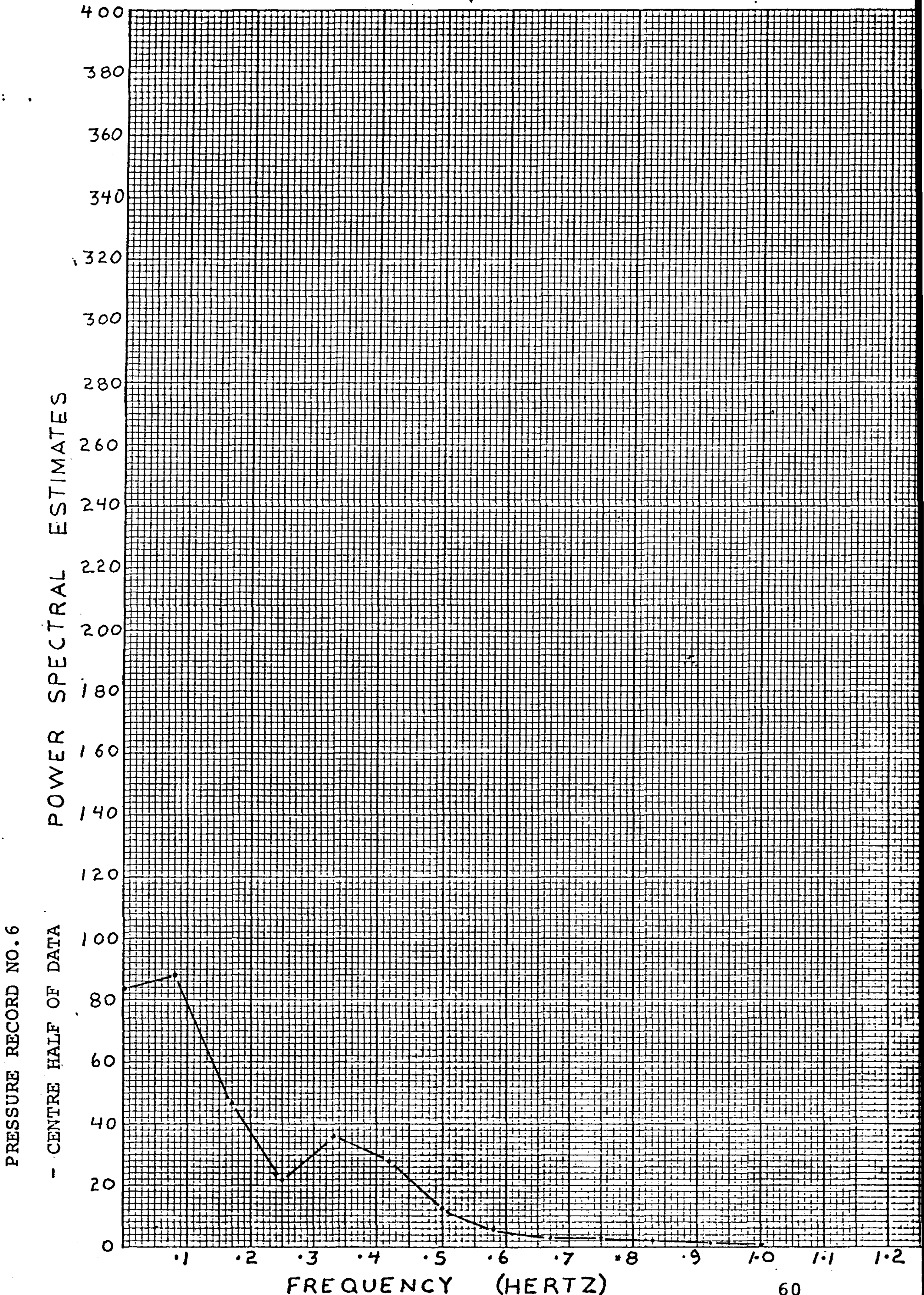

POWER SPECTRAL ESTIMATES
PRESSURE RECORD NO.6
- CENTRE HALF OF DATA
400
380
360
340
320
300
280
260
240
220
200
180
160
140
120
100
80
60
40
20
0
·1
·2
·3
·4
·5
·6
·7
·8
·9
1·0
1·1
1·2
FREQUENCY (HERTZ)

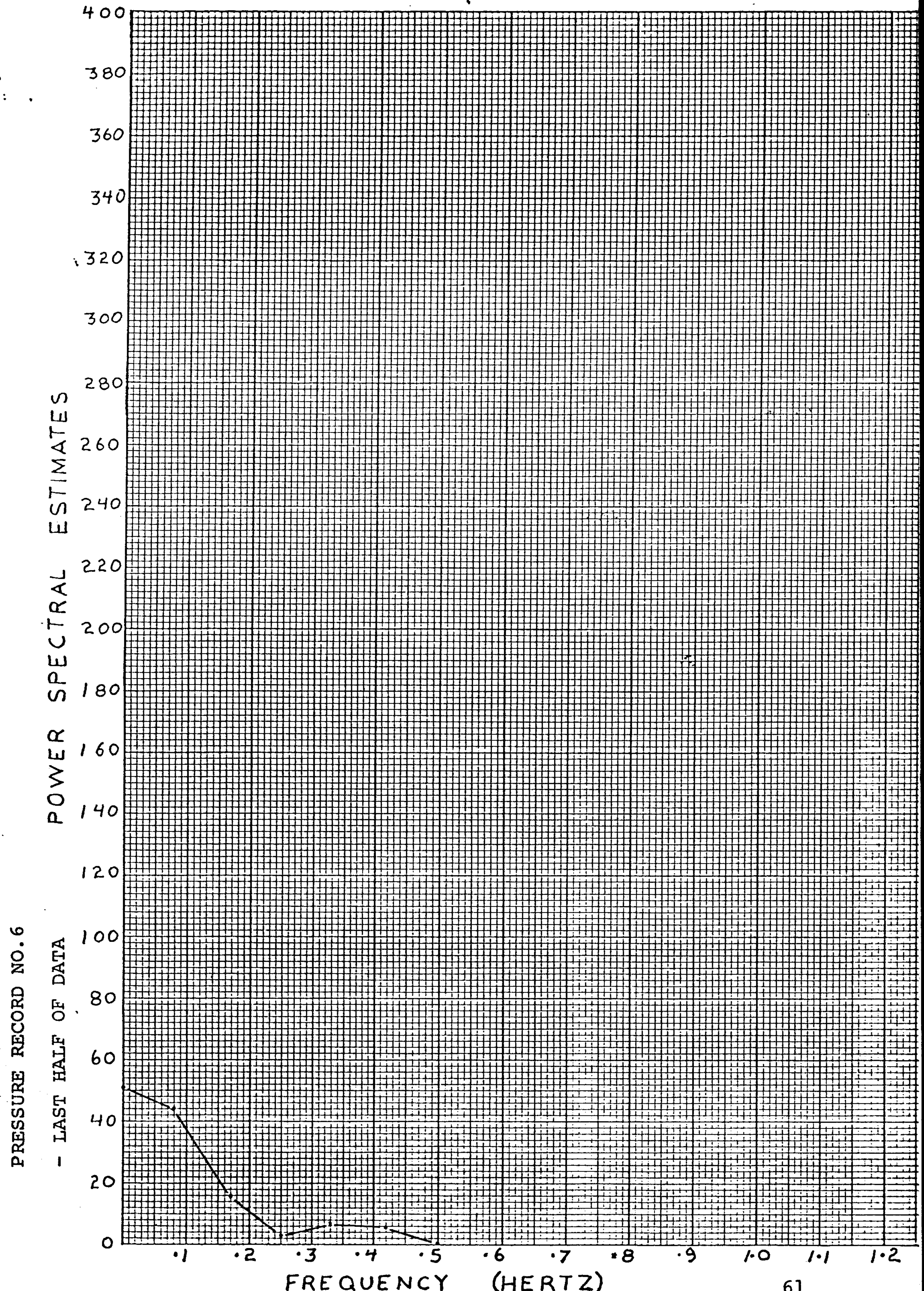

PRESSURE RECORD NO. 6
- LAST HALF OF DATA
POWER SPECTRAL ESTIMATES
400
380
360
340
320
300
280
260
240
220
200
180
160
140
120
100
80
60
40
20
0
·1
·2
·3
·4
·5
·6
·7
·8
·9
1·0
1·1
1·2
FREQUENCY (HERTZ)

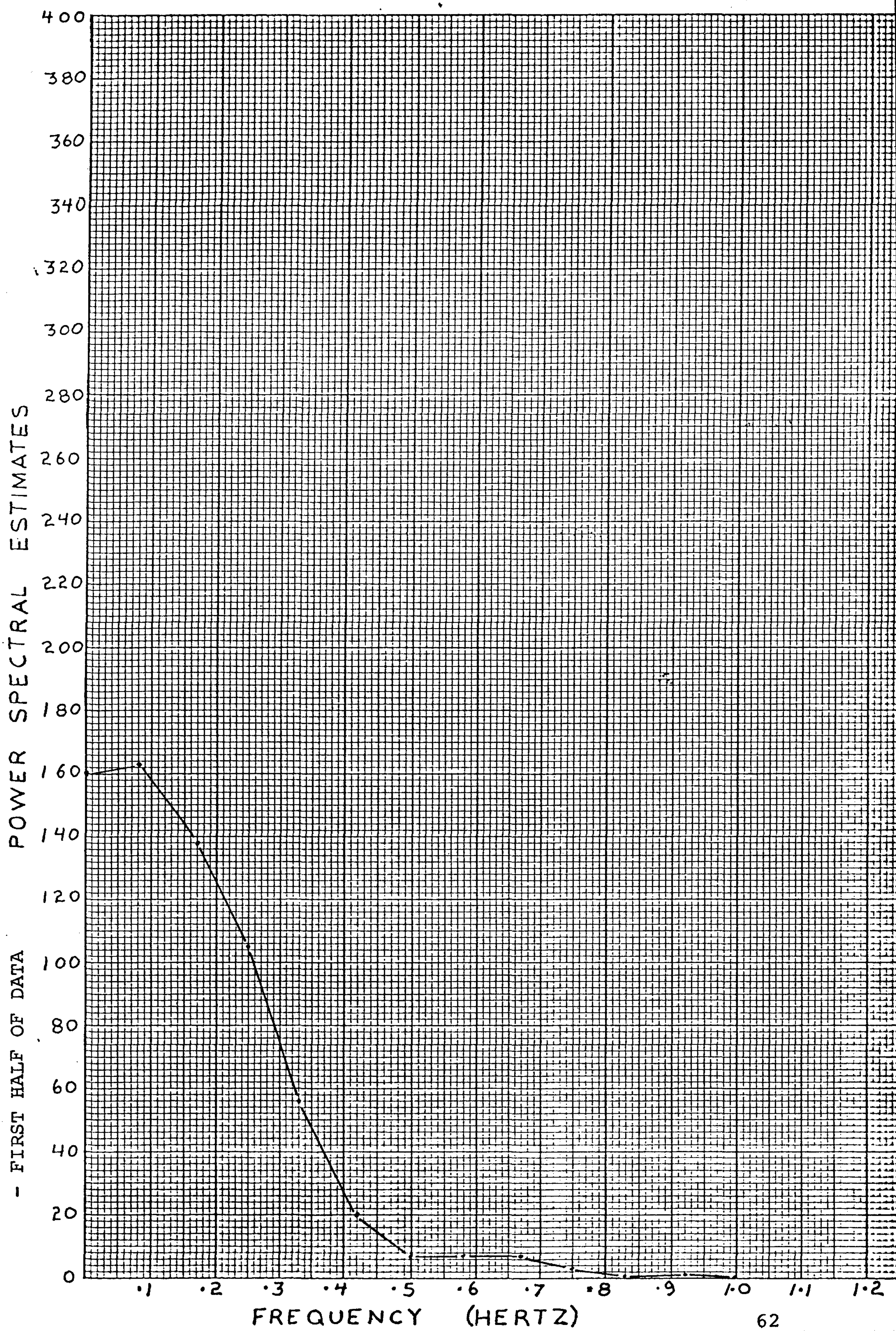

PRESSURE RECORD NO.14
- FIRST HALF OF DATA

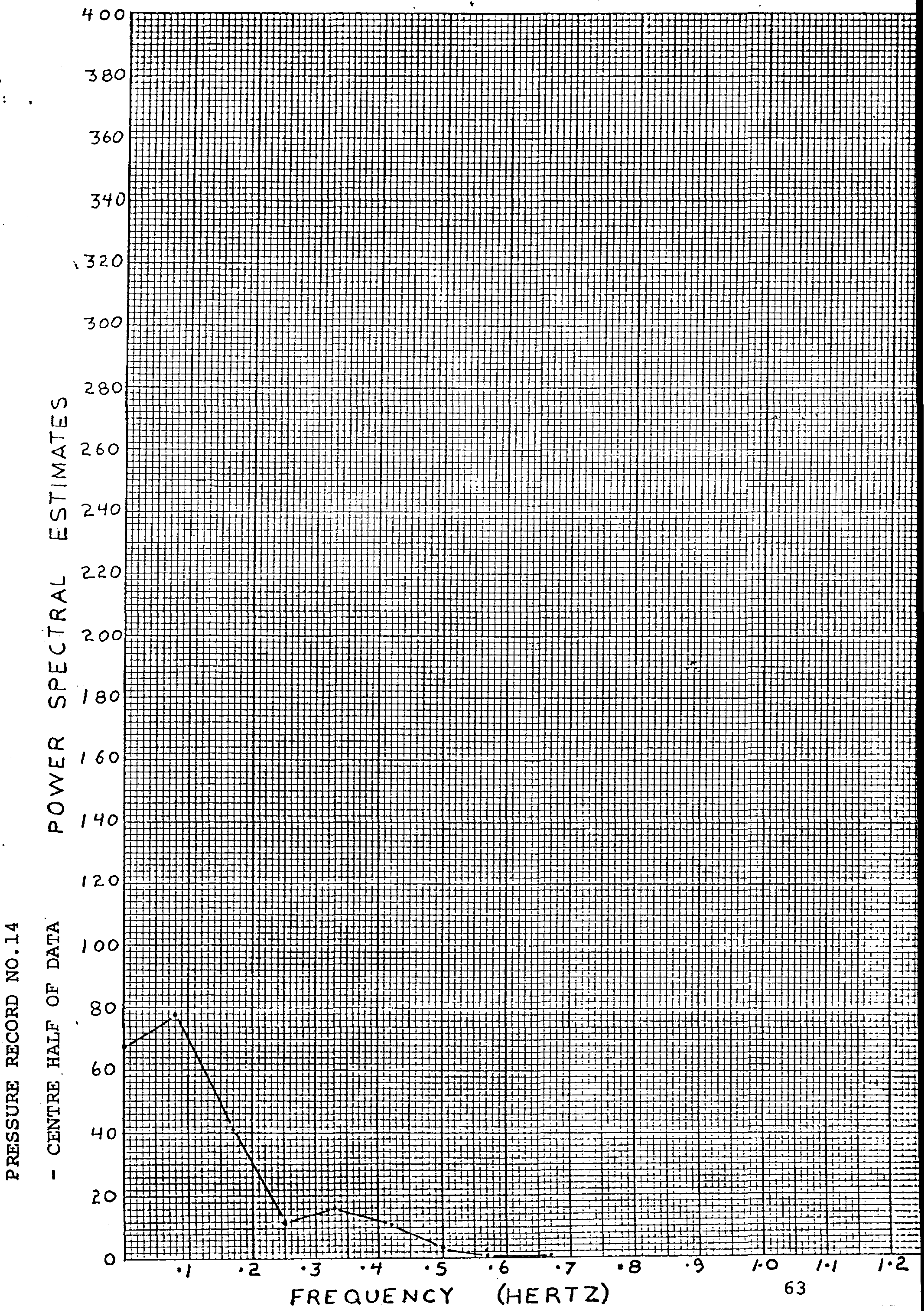

PRESSURE RECORD NO.14
- CENTRE HALF OF DATA
POWER SPECTRAL ESTIMATES
400
380
360
340
320
300
280
260
240
220
200
180
160
140
120
100
80
60
40
20
0
·1
·2
·3
·4
·5
·6
·7
·8
·9
1·0
1·1
1·2
FREQUENCY (HERTZ)

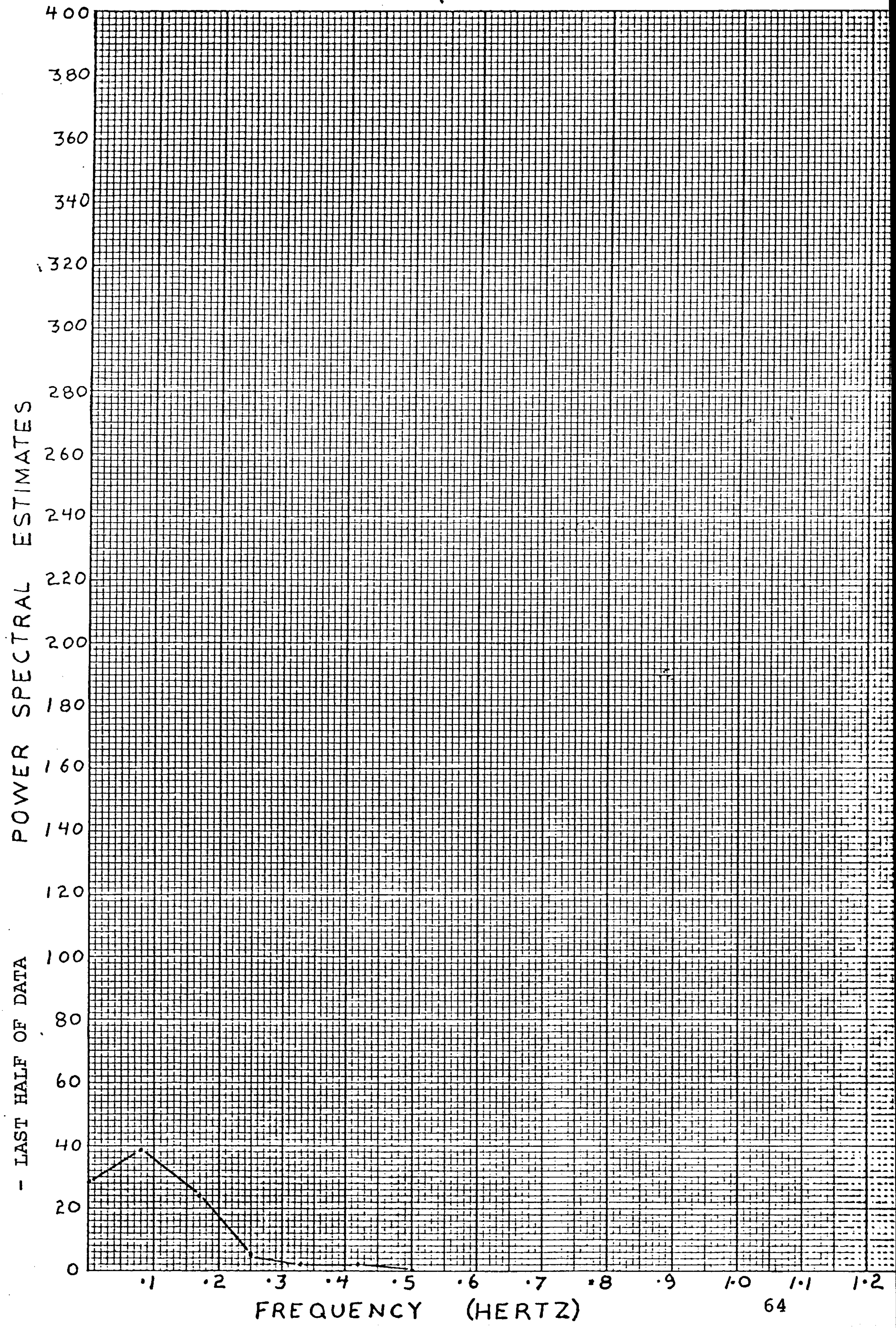

PRESSURE RECORD NO.14
- LAST HALF OF DATA

APPENDIX V

LIST OF ABBREVIATIONS

A	Cross sectional area of pipe
a	Celerity of pressure wave
$C(\tau)$	Autocovariance function
d	Inside diameter of pipe
E	Modulus of elasticity of pipe
e	Base for natural logarithms, 2.71828...
$F_y(\omega)$	Power spectral density
g	Acceleration due to gravity
h	Piezometric head
i	$\sqrt{-1}$
K	Bulk modulus of fluid
L	Length of pipe
$\bar{P}_y$	Total average power of time series
p	Pressure
P_n	Normal operating pressure
Δp	Pressure increment
$S(\omega)$	Single sided power spectral density function
T	Total Time
T_o	Dimensionless time
t	Time
t_1	Thickness of pipe wall
V	Velocity
V_n	Normal operating velocity
V_o	Zero velocity
W	Specific weight of water
X_o	Dimensionless length
x	Length along pipe

$y(t)$	Time series
ρ	Density of fluid
ω	Angular frequency
ω_0	Initial frequency
$\Delta\omega$	Frequency increment
τ	Time lag
∞	Infinity